ELECTROCHEMICAL STUDIES
OF OXIDE-FREE NICKEL SURFACES

by

DARREN LEWIS HENNIG
B.Sc.(Hons), University of Victoria, 1987

A Thesis Submitted in Partial Fulfullment
of the Requirements for the Degree of

MASTER OF SCIENCE

in the
Department of Chemistry

ACCEPTED
FACULTY OF GRADUATE STUDIES

[redacted]
DEAN

DATE 1990-09-10

We accept this thesis as conforming
to the required standard

[redacted]
Dr. D.A. Harrington, Supervisor (Chemistry)

[redacted]
Dr. A.D. Kirk, Departmental Member (Chemistry)

[redacted]
Dr. F.H. El Guibaly, Outside Member (Electrical Engineering)

[redacted]
Dr. A.K.S. Bhat, (Computer and Electrical Engineering)

[redacted]
Dr. T.M. Fyles, Additional Member (Chemistry)

[redacted]
Dr. R.K. Keeler, External Examiner (Physics)

ISBN 0-315-62643-7

Supervisor: Dr. D.A. Harrington

ABSTRACT

The initial stages of oxidation of nickel surfaces in aqueous alkaline solutions and in acetonitrile with trace amounts of water were studied by cyclic voltammetry. To verify that the initial metal surface was free of oxide, a surface preparation method was developed, in which a chemical polishing solution was exchanged *in-situ* by the working solution, while maintaining potential control and oxygen-free conditions. In this way oxide formation from trace atmospheric oxygen or from inadvertent positive potential excursions was avoided. The results using this method on polycrystalline electrodes were compared to those on surfaces prepared by less rigorous electropolishing methods used by other workers. In addition, a single-crystal Ni(111) electrode was prepared, and its behavior was compared to that of the polycrystalline electrodes.

Significant differences in the cyclic voltammetry peak shapes and in the oxidation/reduction charge ratios were found for the different surface preparations, particularly

in the case of the peak for initial oxidation to α-(nickel hydroxide). The results are interpreted in terms of the defect densities of the oxide films, and it is concluded that the films increased in defect density in the order: Ni(111) prepared by the solution exchange method, polycrystalline Ni prepared with the solution exchange method, and polycrystalline Ni prepared with electropolishing. The single crystal surface was found to be about 50% more reactive than the corresponding polycrystalline surface, and this was attributed to favorable epitaxy on the (111) face.

Examiners:

[redacted]

Dr. D.A. Harrington, Supervisor (Chemistry)

[redacted]

Dr. A.D. Kirk, Departmental Member (Chemistry)

[redacted]

Dr. F.H. El Guibaly, Outside Member (Electrical Engineering)

[redacted]

Dr. A.K.S. Bhat, (Computer and Electrical Engineering)

[redacted]

Dr. T.M. Fyles, Additional Member (Chemistry)

[redacted]

Dr. R.K. Keeler, External Examiner (Physics)

TABLE OF CONTENTS

LIST OF TABLES

LIST OF FIGURES

ACKNOWLEDGEMENTS

I would at this time like to thank all the people in the Department of Chemistry at the University of Victoria for their rare qualities of friendship that made the performance of my tasks during my degree program here most enjoyable. I would also like to thank my family and friends for all their support during the "times of need". Lastly, (but not least) I would like to thank my supervisor, Dr. David Harrington, whose support and guidance over the two years of this project has greatly helped in making this thesis possible.

INTRODUCTION

1.1 - Introduction.

The importance of nickel, both in catalytic systems and also in battery technology, has been known for some time. The surface electrochemistry of Ni, particularly in aqueous solutions, is still a subject of considerable study. This is mainly due to the fact that nickel metal is sufficiently reactive in solution that it can form various mixed oxides on its surface, whose stoichiometry itself is a subject of considerable debate in the literature. One possible reason for the variability in the literature results discussed below, is that the surface preparation method used may lead to a surface which is not clean and oxide-free prior to beginning the experiment. Accordingly, in this work a surface preparation method was developed, in which a chemical polishing solution was exchanged *in-situ* by the working solution, while maintaining potential control and oxygen-free conditions. In this way oxide formation from trace atmospheric oxygen or from inadvertent positive potential excursions should be avoided. A cyclic voltammetry study was then carried out to compare the initial oxidation behavior for the various surfaces. In addition, a single-crystal Ni(111) electrode

was prepared, and its behavior was compared to that of the polycrystalline electrodes.

There is a substantial literature concerning the nature of the various nickel oxides and hydroxides, and their electrochemical formation on nickel surfaces. Bode, Dehmelt and Witte [1] were the first researchers to study anodic oxidation of Ni in detail, and the formation of various oxide phases was the main area of their research. They studied the various phases using X-ray crystallography and using elemental analysis, and came up with the following reaction scheme for the oxide phases formed on Ni in alkaline aqueous solution:

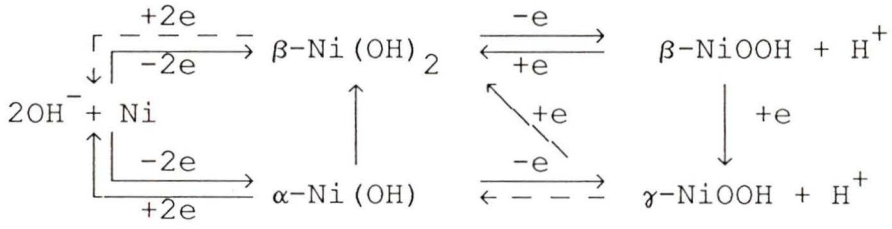

The above reaction scheme has been appropriately named 'the Bode diagram', and is still considered the most representative electrochemical reaction scheme for Ni in aqueous solution.

Many of these oxides have been characterized by other researchers [2,3] as well. A fairly recent review by Oliva

et al [4] describes the electrochemistry of the nickel aqueous system in the following way: "The α-$Ni(OH)_2$, as seen above, is the kinetically favored hydrated oxide (or hydroxide), and is fully reducible back to metallic Ni. A second hydroxide, the β-phase, or β-$Ni(OH)_2$, is the thermodynamically favored phase, and is irreversibly formed from both bulk Ni and the α-OH due to the electrochemical 'aging' of the α-phase upon cycling the potential of the system. Early crystallographic studies [5,6] established a marked distinction between the "well crystallized" β-$Ni(OH)_2$, isomorphous with brucite, $Mg(OH)_2$, and compounds which can still be considered as Ni(II) hydroxides but which contain a variable excess of intersheet water and foreign ions, and exhibit relatively low crystallinity. The conventional α-$Ni(OH)_2$ terminology for such compounds has been thus taken as a general denomination for a large set of disordered Ni(II) hydroxides and does not represent a well defined polymorph of $Ni(OH)_2$. The similarity of the trends observed in the electrochemical behavior of all hydroxides with those produced chemically has induced electrochemists to adopt the same type of nomenclature as the crystallographers." The α-hydroxide can be *chemically* transformed to the β-hydroxide by the repairing of defects in the film as it is produced to form a more highly

crystallized film on the surface. The well-defined β-phase is then obtained.

1.2 - Structures of Nickel Hydroxides and Oxyhydroxides

The well characterized β-$Ni(OH)_2$ is a hexagonal system ($P\bar{3}m1$), common to several alkali metal hydroxides as well as to the structure of CdI_2. This is displayed schematically in figure 1 [7]. The unit cell parameters are a = 3.126 Å and c = 4.605 Å. [4]. The structure of the β-OH above can be described as a "hexagonal close-packed structure of hydroxyl ions (AB oxygen packing) with Ni(II) ions occupying octahedral interstices in one plane out of two. It can also be visualized as a layered structure, each layer consisting of a hexagonal planar arrangement of Ni(II) ions with an octahedral coordination of oxygen, three atoms lying above the Ni plane, three lying below. The layers are stacked up along the c axis and the O-H bond is thought to be parallel to the c axis. There is no hydrogen bonding between the OH groups of two adjacent layers." [4] This is seen in IR data by Cabannes-Ott [8], which shows exclusively a peak at 3650 cm^{-1}, which is attributed to the characteristic stretching vibrations of non-hydrogen-bonded hydroxyl groups.

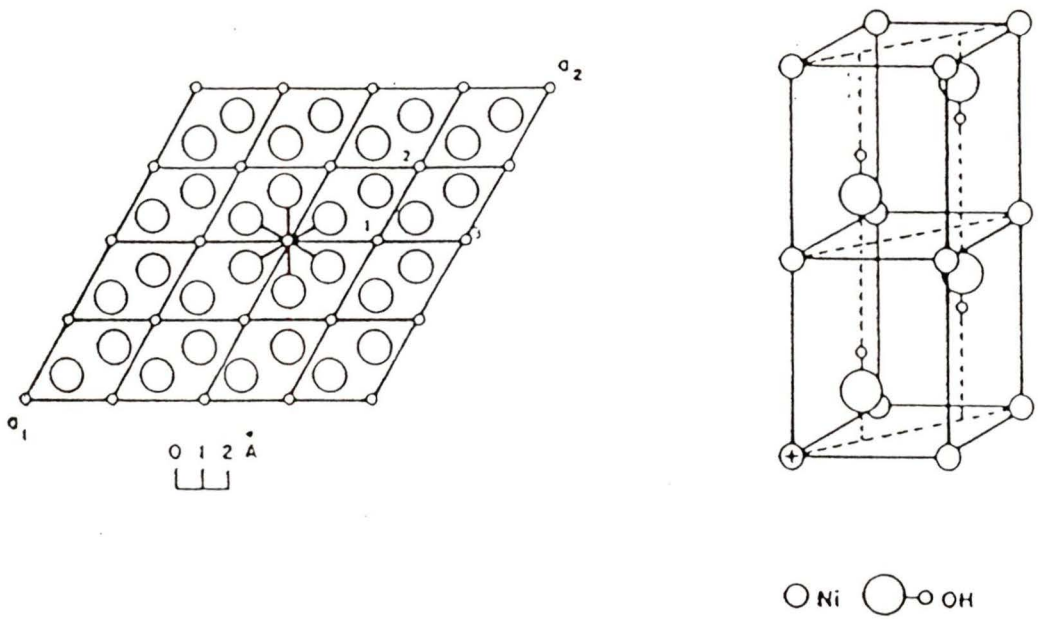

Figure 1: Structure of the β Form of Nickel Hydroxide

1.3 - Oxidation States in the Hydrated Oxide Films.

The oxidation state of Ni in the β-OH phase is two. However, according to Oliva [4]: "by continuously cycling the potential of the system through the entire range, an average value of 2.3 for the oxidation state of Ni in the β-phase is obtained. The 2.3 figure is an accepted one in the literature and can be interpreted as the existence of Ni(III/IV) defects in the lattice which would give increased conductivity of the hydroxide phase. The band structure of β-$Ni(OH)_2$ leads to the rather poor observed electronic conductivity, this being mainly due to the Ni-Ni intercationic distance of 3.12 Å. The presence of these impurities shorten the bond length to about 2.99-3.04 Å which tends to favor better orbital overlapping and hence provides a reasonable explanation for the observed increase in conductivity during continuous cycling of the potential in voltammetry studies [1,2,9]."

Upon oxidation of the hydroxide phases, the average oxidation state for the Ni cations goes from 2.3 to 3.3. [4]. The β and γ-oxyhydroxides are known to be the oxidation products of the β and α-phases respectively, as seen on the Bode diagram above. The structure of these higher oxides is

known to be quite similar to that of the β-OH phase on Ni [4], and will be discussed further later on. There has been considerable debate as to the structural and chemical variations which exist in the higher oxides, particularly by earlier researchers [1,3,11-13]. As seen below, MacArthur [14] shows in his paper the variations in higher oxide stoichiometries employed in previous studies of α and β-OH oxidation to demonstrate the difficulties in finding a mechanism for their formation:

$$2Ni(OH)_2 \cdot 1.28H_2O + 0.14KOH + 2OH^- \rightleftharpoons 2NiOOH \cdot 0.14KOH + 4.56H_2O + 2e^-$$

[Bourgault and Conway, 3]

$$2Ni(OH)_2 \cdot 2H_2O + 2OH^- \rightleftharpoons 2NiOOH \cdot H_2O + 4H_2O + 2e^-$$

[Zedner, 11]

$$2Ni(OH)_2 + 2OH^- \rightleftharpoons 2NiOOH \cdot 0.2H_2O + 1.8H_2O + 2e^-$$

[Forster, 12]

$$2Ni(OH)_2 + 2OH^- + 0.067KOH \rightleftharpoons 2NiOOH \cdot 0.067KOH \cdot 1.16H_2O + 0.84H_2O + 2e^-$$

[Kornfeil, 13]

Melendres' discussion [10] on the structure of the higher oxides of Ni clearly shows crystallographic and IR/Raman evidence that the structures of these oxides are similar to

that for β-OH. Both types of oxyhydroxide phases may adopt hexagonal or rhombohedral structures, depending on their water content and the amounts of deprotonated hydroxide (or oxide anions) present in the lattice. The Ni-Ni bond distance in γ-OOH is about 2.86 Å, which clearly indicates the existence of many Ni(III/IV) sites in the lattice. These sites provide significant orbital overlap between metal atoms. It has been suggested by Melendres [10] that the pathway by which the hydroxides are oxidized may proceed mainly via proton abstraction at the hydroxide sites in the crystal. This is also supported by the review by Oliva [4], which shows crystallographic evidence for layer slippage upon oxidation. He suggests the following: Upon oxidation of β-OH, β-OOH, which has the same ABA packing, is first obtained. Further oxidation to the γ-OOH implies that electrons are removed from Ni^{3+} ions (giving Ni^{4+}) as well as protons from the intersheet hydroxide moieties. At the same time water is intercalated, some of the remaining protons are exchanged by alkali metal ions, and a sheet glide occurs. This is shown schematically in figure 2. A consequence of the structural rearrangement is an increase in the intersheet distance from 4.85 Å (β-OOH) to 7 Å (γ-OOH). This is approximately the size of a water molecule, and supports the above proposed mechanism. Unfortunately,

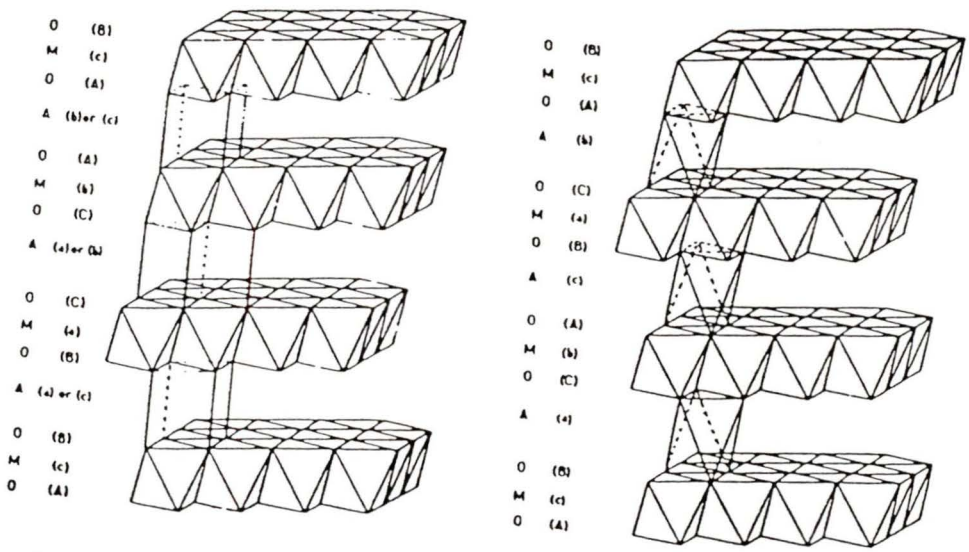

Figure 2: Structural Changes Occurring During Oxidation of β-NiOOH to γ-NiOOH (Oxygen Packings are ABCABC and ABBCCA) (from ref. [4])

Table 1: Reversible Potentials for Nickel Oxides and Hydroxides (data from ref.[15], except for (iv) and (v) from [4])

(i) $Ni^{2+} + 2e^- \longrightarrow Ni$

$E_{rev} = -0.236V + 0.0296 \log [Ni^{2+}]^*$ (-0.414V @ pH 14)

(ii) β-$Ni(OH)_2$** $+ 2H^+ + 2e^- \longrightarrow Ni + 2H_2O$

$E_{rev} = 0.140V - 0.0592$ pH (-0.689V @ pH 14)

(iii) $NiO + 2H^+ + 2e^- \longrightarrow Ni + H_2O$

$E_{rev} = 0.132V - 0.0592$ pH (-0.697V @ pH 14)

(iv) γ-$NiOOH + H_2O + e^- \longrightarrow \alpha$-$Ni(OH)_2 + OH^-$

$E_{rev} = 0.295V - 0.0139$ pH (+0.100V @ pH 14)

(v) β-$NiOOH + H_2O + e^- \longrightarrow \beta$-$Ni(OH)_2 + OH^-$

$E_{rev} = 0.501V - 0.0028$ pH (+0.462V @ pH 14)

(vi) $O_2 + 4H^+ + 4e^- \longrightarrow 2H_2O$

$E_{rev} = 1.229V - 0.0592$ pH (+0.400V @ pH 14)

(vii) $2H^+ + 2e^- \longrightarrow H_2$

$E_{rev} = 0.00V - 0.0592$ pH (-0.829V @ pH 14)

(all potentials calulated versus the SHE (E = 0.000V))

*$[Ni^{2+}] = 10^{-6}$M (assumed)

**The β-phase is the only thermodynamically stable hydroxide.

because of the complex conversion of phases during oxidation, kinetic studies on the system are very difficult to perform.

1.4 - Thermodynamics of Formation of Nickel Oxides and Hydroxides

The reversible electrode potentials for formation of the various oxide and hydroxide phases may be calculated for the experimental conditions using the Nernst equation. The E° values required may be calculated from free energies of formation (ΔG_f°), if they are not available directly. Some assumption or measurement of the activity coefficients in the solutions is also required. Table 1 shows reversible potentials, calculated from tables of E° and ΔG_f° [15] assuming activities equal to concentration. Numerical values are given at pH 14 (appropriate for the 1M NaOH used) and the concentration of Ni^{2+} near a dissolving electrode is arbitrarily taken to be 10^{-6} M.

These calculations allow tentative identification of the experimental cyclic voltammetry peaks. However, there is little reliable data for the non-stoichiometric phases. so these numbers are at best a guide. It must also be

remembered that kinetic factors cause oxidations to appear at more positive potentials than the reversible potential, and reductions to appear at more negative potentials. Accordingly, these values provide only an approximate guide for interpreting the cyclic voltammetry data.

1.5 - Cyclic Voltammetry Behavior in Alkaline Aqueous Solutions.

The kinetics of nickel electrode oxidation have also been studied in great detail, but, depending on which phase is considered, the kinetic expressions governing each phase-forming process vary in their mathematical forms. A typical nickel cyclic voltammogram is seen in figure 3, and will help to illustrate the above points. What is believed to be occurring on a polycrystalline nickel electrode can be described as follows: The first oxidation peak α' (a shoulder on the negative potential side of peak α-OH in figure 3) is attributable to oxidation of either adsorbed hydrogen to H_2 [2] or of Ni to soluble Ni^{2+} [17]. In peak α-OH, nickel is oxidized to the α-$Ni(OH)_2$ phase. This phase may be irreversibly converted to a β-OH phase at higher potentials (β-OH in figure 3) in a process which is not yet fully understood. Both residual α-OH and the newly-formed

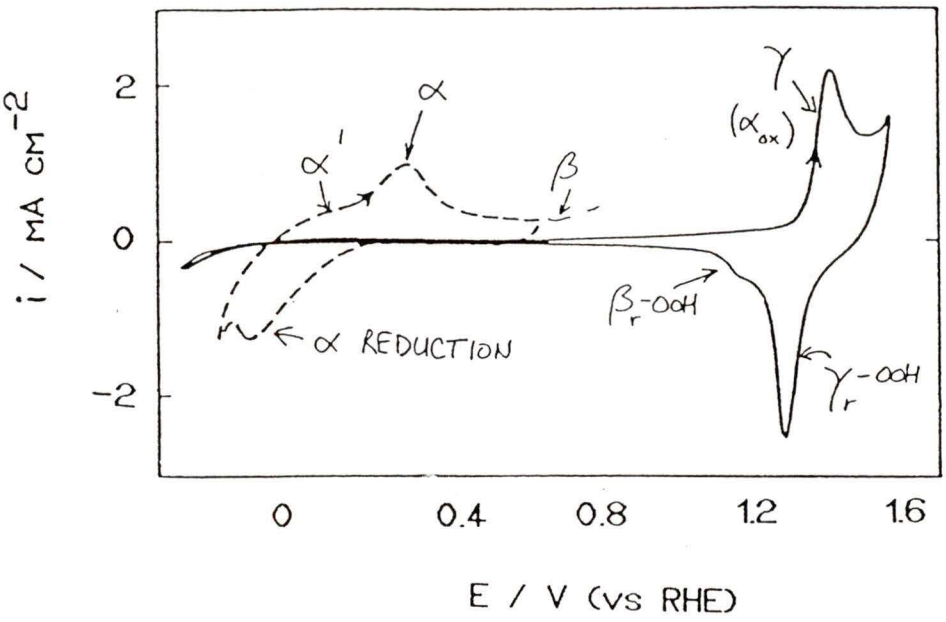

Figure 3: Typical Cyclic Voltammogram of Nickel in 1M NaOH (from ref. [2], with change of potential scale to RHE)

β-phase may be reversibly oxidized to β- and γ-Ni(OOH) in the peak denoted γ in figure 3. These oxyhydroxides of nickel have very complex stoichiometries, as mentioned previously, depending on their water content. They have an average Ni oxidation state of 2.9 to 3.4, depending on their formation conditions (e.g. surface cleanliness, electrolyte concentration, impurity levels, etc.)

When the potential is increased beyond that for γ-OOH formation, the oxygen evolution reaction (O.E.R) and surface roughening begins in the region beyond the limit of Figure 3. Upon reversing the sweep, the β and γ-OOH phases can be reversibly reduced to the α and β-OH phases in a single prominent reduction peak with a long tail. No significant feature is then observed until the α-OH reduction peak where the surface α-OH phase reduces back to Ni. This is followed by the hydrogen evolution reaction (H.E.R.) as water becomes reduced at the electrode.

The seemingly simple aqueous electrochemistry exhibited by Ni is misrepresentative, since features such as the interference of the H(ads) oxidation peak by the α-OH phase formation peak make kinetic studies of that reaction difficult. Moreover, the lack of resolution of the β-OOH and

γ-OOH formation peaks shows the rather ill-defined stoichiometry of these phases. Before any full conclusions can be drawn as to the kinetic behavior of Ni in the various potential regions, the surface reactions described above must be more thoroughly characterized.

Most of the work performed on the nickel electrode to date has been involved with trying to understand the kinetics of hydroxide formation (α-OH mainly) [2,18] and the studies involving cycling in the β and γ-OOH regions [2,18,19] in an attempt to understand the kinetics of the Ni system in that potential region. Many researchers suggest that the α to β-OH conversion process proceeds via a first order mechanism [1,3,14]. Unfortunately, the overlap of the β-OH plateau with the tail end of the α-OH peak makes it difficult to determine where the α-OH formation ends and the β-phase begins. This leads to significant complications in the kinetics when attempting to do a detailed study. Studies of β-OH oxidation reaction(s) to β and γ-OOH have been more successful. However, the majority of research in this area has dealt with capacitance studies and charge retention with cycling, which has more significance in the battery technology applications of this research than in extending the knowledge on the kinetic behavior of Ni in this

potential range.

Some very limited work has been performed on Ni single crystal electrodes in alkaline aqueous solution to date. Weininger and Breiter [2] did the preliminary work on the anodic oxidation of the three Ni low index planes and found that the extent of oxidation depended on the nature of the crystal face studied. The most open of the faces, the (110) plane, exhibited the most extensive oxidation as measured by the amounts of charge required during the positive potential sweeps. Beden *et al* [20] have performed work using the three lowest index Ni crystallographic planes as their electrodes. The only structural effects observed were differences in the formation kinetics of the α-OH phase and its subsequent reduction. All other aspects of the systems were qualitatively identical to those observed with polycrystalline Ni electrodes. He was, however, more careful in his preparation of the surface. His method involved polishing the electrode surface to a 0.05μm finish with alumina slurry and transferring the newly polished electrode to the electrochemical cell by protecting it with a droplet of de-oxygenated H_2O. The main problems with his surface preparation are (1) that transfer through atmosphere may allow any O_2 present to diffuse through the protective drop

towards the surface, causing premature oxidation of some or all of the surface, and (2) that the surface is likely still rough on the atomic scale, since no high temperature annealing was done.

Some advancements over previous studies of single-crystal nickel electrodes were achieved by Wagner *et al* [21]. His use of ultra-high vacuum (UHV) techniques in the study of the Ni(100) system enabled a direct comparison between an electrochemically grown NiO film, and one formed by direct O_2 dosing of the clean Ni surface. The surface was cleaned using Ar^+ ion bombardment and, at times, heating in H_2 to remove recalcitrant oxide from previous experiments. Vacuum annealing of the surface at 900K was also done. The electrode condition was always checked by Low-Energy Electron Diffraction (LEED) to ensure good surface order. The main investigative tools were X-ray Photoelectron Spectroscopy (XPS), High Resolution Electron Energy Loss Spectroscopy (HREELS), and LEED. Although this study was done in aqueous $HClO_4$, some very interesting features were prevalent in the data. The XPS data showed a large degree of similarity between the films grown electrochemically and by dosing. Both showed O(1s) signals very close to 529.4eV. On rinsing, the passive film which was electrochemically-grown

at 1.05V vs RHE, showed peaks at 531.2eV and at 532.2eV. The first extra peak accounted for 40% of the total signal and was attributed to OH groups in or on the passive layer. Some of this may also be higher oxides (e.g.: Ni_2O_3), since O_2 was released on heating to 700K and was *not* observed when the dosed surface was heated. Some trace ClO_4^- was also observed to exist in the electrochemical film (evidenced by the presence of Cl XPS signals). XPS data and impedance experiments showed the passive layer was about 6.8Å thick, in agreement with other literature values [22]. The film thickness was deduced from electron attenuation parameters for XPS. Total charge in contact coulometry experiments was attributed to dissolution of Ni *and* film formation in the acidic medium used as the electrolyte, when the total charges passed for the oxidation of the dosed surface are compared to those for an initially clean surface.

The LEED data showed clear distinctions between the epitaxial arrangement of oxide in the surface doped film and the electrochemical film. NiO in the (100) orientation was the *only observed* epitaxy for the doped film. The epitaxy of the NiO layers in the electrochemically-grown film were of a (111) film only. The doped film retained its (100) epitaxy even on exposure to electrolyte, whereupon the chemical

composition approached that of the electrochemical film, as seen by XPS.

There has been very little work done in utilizing oxide-free, well-defined Ni surfaces for studying their initial electrochemical oxidation, especially in non-aqueous systems. Although there have been attempts to inhibit, or at least alter, the oxidation reactions on Ni, there still is some doubt as to the care taken by previous researchers in maintaining an oxide-free surface prior to an experiment. All previous researchers have used mechanical polishing or electropolishing/chemical etching methods to prepare their electrodes for study. The problem that these methods have is that they expose the electrodes for a finite time to an atmosphere which may contain sufficient gaseous O_2 to cause the preliminary oxidation of the surface. This may have a detrimental effect on the electrode surface, since small coverages of oxide may invalidate experimental results by roughening the surface as well as providing sites for oxidation to continue, thus altering the entire system being studied. This is especially important in the single crystal studies, since oxide formation leads to the disordering of the surface, thus affecting the reactivity of surface sites.

The approach taken by Wagner *et al* [21] in attempting to obtain an oxide-free, well ordered surface appears to be satisfactory, since he observes associative adsorption of H_2O on the surface prior to running his oxidation reactions. It is known from high pressure surface studies on polycrystalline Ni [23] that H_2O can dissociatively adsorb on the surface. Wagner's work is the first example in the literature of an oxide-free surface acceptable for performing Ni oxidation studies. There is no reason to believe that the more stable (111) surface should *not* be similar to the (100) surface studied by Wagner in its reactivity towards water. The (110) surface, however, may be more highly reactive and may dissociatively adsorb H_2O, if one takes the data from Weininger's study [2], as suggestive of this. He showed that the (110) surface is more reactive and behaves more similarly to polycrystalline Ni than any of the other low-index planes of Ni. This could lead to oxidation of the surface *before* it has been electrochemically treated. This may lead to disorder on the surface prior to any of the intended experiments, and hence may alter the results from those for a clean, oxide-free surface. Wagner's surface preparation procedure may *not* be satisfactory for more reactive single crystal surfaces, since it still allows for the exposure of the surface to an

oxidative environment (i.e. water vapor) before the performance of an electrochemical experiment.

As a result of this apparent lack of care in surface preparation techniques in the study of nickel electrodes to date, there is a great need to characterize the surface of the electrode under study while maintaining its structural integrity, regardless of the crystal face studied. Furthermore, there are still sufficient inconsistencies in the literature which require rectifying before a clear picture of oxidation reactions occurring at a nickel surface can be drawn. Further studies on polycrystalline electrodes are required, as well as more detailed studies of the three low index planes of Ni. Of particular interest are studies in which the preliminary onset of oxidation and disorder at the surface are minimized or eliminated. An experimental technique to avoid the onset of oxidation prior to the study is required. This would then generate a well-defined initial electrode surface condition suitable for oxidation studies. In the rest of this work, such a method is discussed.

EXPERIMENTAL

2.1 - Fluid Transfer Procedures for the Aqueous Studies.

The following procedure was developed to ensure that the surface of the Ni working electrodes was maintained in an oxide-free condition, and that the electrode was under potentiostatic or galvanostatic control at all times. It involved *in-situ* solution exchange from an electropolishing solution to the 1 M NaOH working solution. This replacement (which will be referred to here as an elution) was done as follows:

The cell was filled with the electropolishing solution to a volume of about 40mL. The polishing solution consisted of 2:1 conc.H_2SO_4: H_2O (final conc.= 67% v/v). The Ni working electrode was electropolished galvanostatically at about 250-400$\mu A/cm^2$, which yielded fairly vigorous O_2 evolution at the working electrode. After two minutes of polishing, the cell was isolated at open circuit for about 4.5 minutes, after which the open-circuit potential had stabilized. This step was designed to remove the 6-9Å of oxide left during the polishing step, as suggested by Macdougall [22]. The electrode was then potentiostatically held at -200mV (vs

RHE* - in the H_2 evolution region) to maintain the integrity of the electrode surface during elution. The fluid in the cell was then switched slowly to the electrolyte (1.0 M NaOH).

This is accomplished by an elution procedure (see figure 4), with the electrolyte (solution purged by Ar and kept under Ar) being fed via tubing into the cell (at 1.2 mL/s) under a slight positive pressure. The cell was drained at the same rate, leading to no net change in solution volume. The cell turnover time was about 10 minutes for approximately 99.9% complete replacement of polishing solution by electrolyte.

The working electrode was kept under constant potentiostatic control during the entire elution procedure. During a typical run, no net anodic current was observed, suggesting that no oxidation of the metal surface had been performed.

---

* RHE = *Relative Hydrogen Electrode;* i.e. a hydrogen electrode in the working solution; its potential is pH dependant.

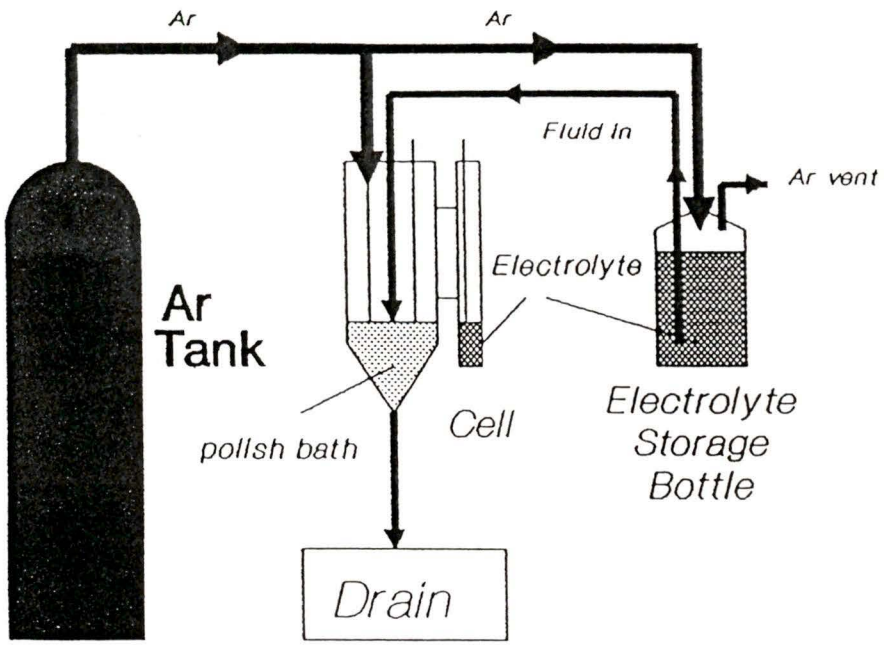

Figure 4: Apparatus Used in Elution Procedure

2.2 - Glassware and Electrode Cleaning Procedures.

All glassware was cleaned thoroughly in a concentrated CrO_3/H_2O bath, kept at a temperature of about 65°C. The glass surfaces of the cell were bathed completely by the bath and left in for about 5 minutes to ensure the complete oxidation of any adsorbed organic residues. The bathed components of the cell were then flushed thoroughly with ultra-pure H_2O (Millipore; Milli-Q system), and left in a fume hood while other components were cleaned. The cell was assembled systematically while cleaning. After being rinsed, a newly-cleaned component was assembled in the appropriate position on the cell. For the experiments involving acetonitrile as a solvent, the complete cell was then put into an oven at 120°C until dry, and cooled in a dessicator until required. A diagram of the electrochemical cell employed in this set of experiments is shown in figure 4.

2.3 - Single Crystal and Disk Electrode Preparation Procedures.

The polycrystalline disk electrode employed in these experiments consisted of a Ni rod (Johnson-Matthey; 99.998% pure) 0.5cm in diameter and 0.5cm long, mounted in a teflon

holder 2.5cm high (see figure 5.). The electrode was prepared by firstly smoothing the surface using 600 grit SiC paper, then 1500 grit paper. This allowed the surface of the Ni to be coplanar with the flat teflon base of its holder. The surface was then polished on a lapping wheel turning at a rate of about 50rpm. Polishing cloths were employed (Beuhler) and were laden with 6μm diamond paste. Heavy liquid paraffin oil was used as a paste extender. This aided the polishing process by both lifting the diamond particles continually, and acting as a coolant/lubricant to prevent buffing. The final stage involved a very gentle polish obtained by putting the electrode into a 0.05μm alumina slurry in a vibratory polishing machine. This gave a surface of very high quality. Care had to be taken though, because previous work on our electrodes suggested that if the surface was not under constant motion in the slurry, the surface would become highly mottled, resembling an orange peel in its appearance.

The Ni(111) single-crystal electrode was prepared under very similar conditions to that of the disk electrode. The major differences between the preparations of the two

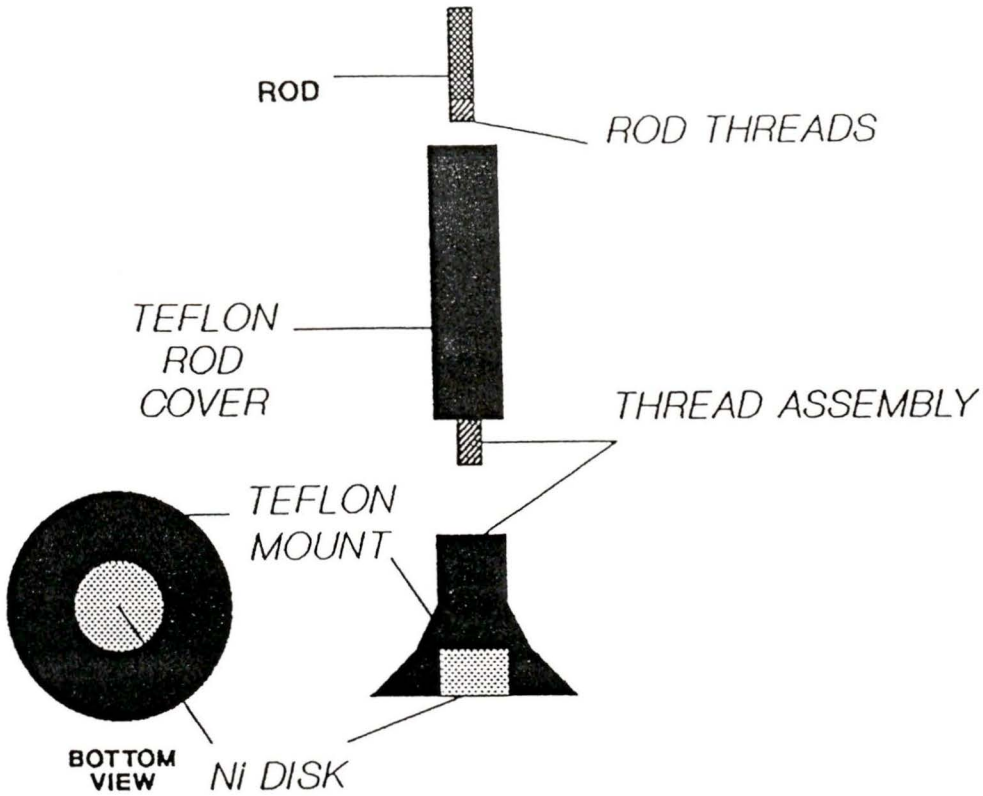

Figure 5: Rotating Disk Electrode Assembly

electrodes were that the surface orientation of the crystal needed to be maintained at all times during the polish procedure, and that the crystal had to be polished under much more care to ensure that surface disorder was not incurred upon polishing.

The crystal was cut from a boule of high purity nickel (Metal oxides and crystals, Ltd., Cambridge, U.K.; 99.999% purity). The boule was mounted in transparent dental acrylic (Lang's Jet repair acrylic), and the leading face was polished to 6μm using diamond paste. Back-Laüe X-ray diffraction was then used to orient the boule to the crystallographic face of interest ((111) in this case; see figure 6). Once oriented, the crystal boule was transferred to a low-speed diamond saw. The arm holding the boule was designed to preserve the crystallographic orientation upon transfer to the saw. The crystal was then cut slowly over about 3 days. The original thickness of the crystal was about 2.5mm after cutting. The crystal was then cleaned in dichloromethane to remove the acrylic still surrounding the crystal. The cleaned crystal was then re-mounted in acrylic and put on a polishing jig using paraffin wax (see figure 7). The surface was smoothed by treatment with SiC paper. The jig was then set up on the lapping machine arm which was designed to oscillate at a rate of 15 sweeps per minute,

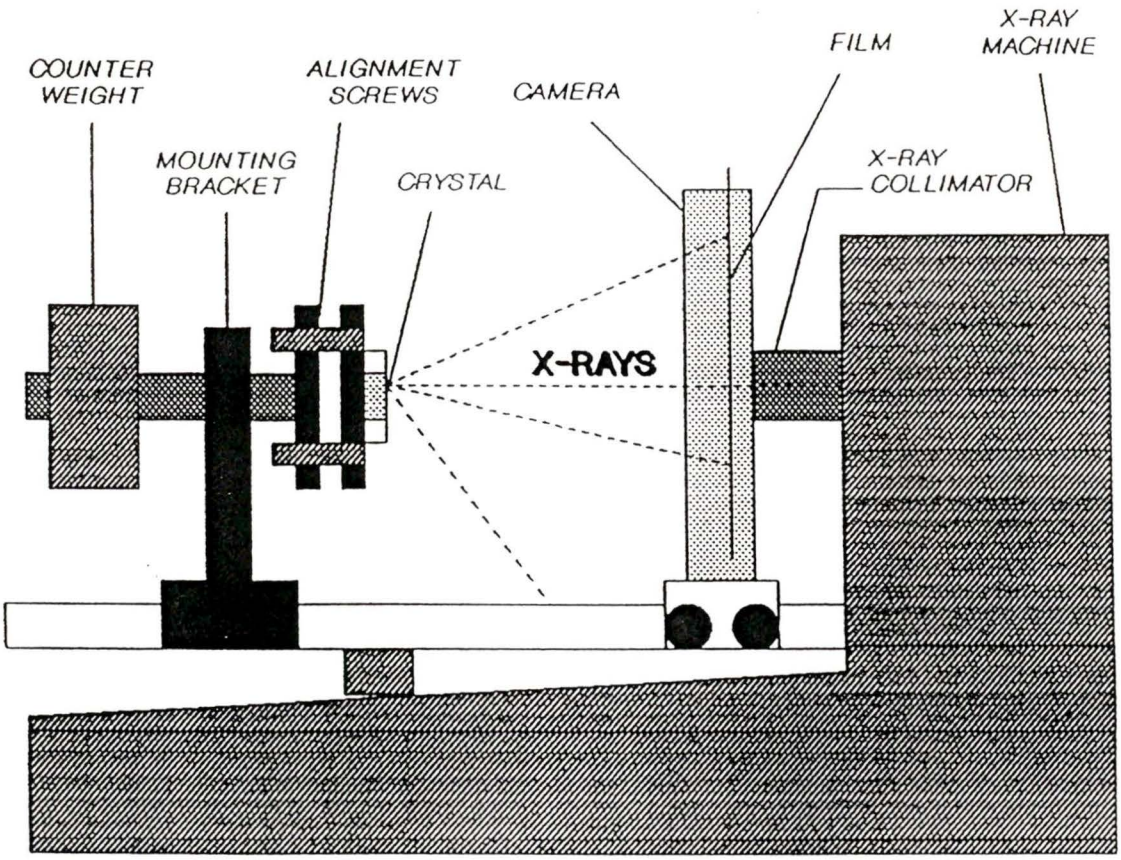

Figure 6: Apparatus for Back-Laüe Alignment of the Ni(111) Single Crystal

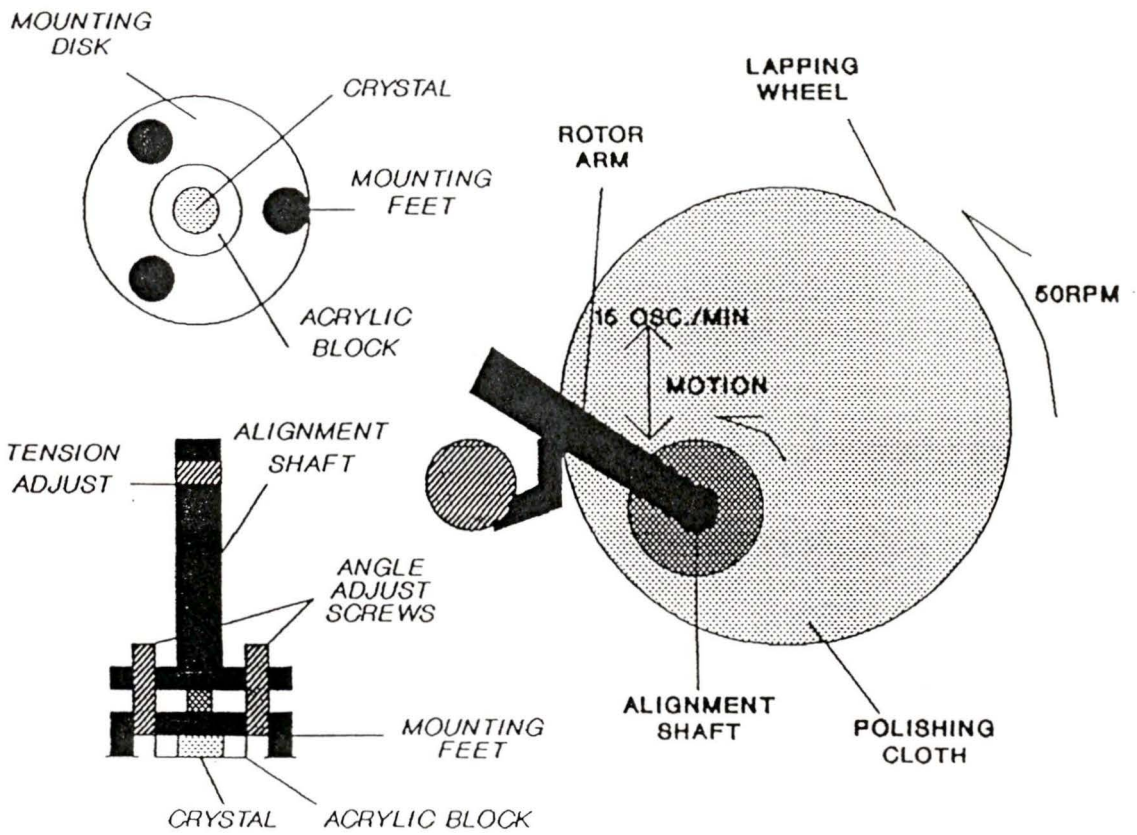

Figure 7: Mounting Jig and Polishing Apparatus for Preparation of Ni(111) Single Crystal

while the cloth rotated underneath at 50rpm (see figure 7). This arrangement permitted very uniform polishing over the entire surface. The crystal was in contact with the cloth under minimal pressure to prevent buffing the surface. The crystal orientation was checked on the X-ray machine after polishing to 6μm to ensure the orientation was preserved. Typical X-ray operating parameters were 27kV at 20mA and 20 minute exposures on Polaroid type 57 film (3000 ASA). The X-ray camera used was a Polaroid XR-7 Back-Laüe Camera. Once re-aligned, the crystal was taken through a repeat treatment with the sanding paper and the 6μm diamond paste. The alignment was once again checked, and was within 0.5° of the required (111) orientation. The crystal could then be carried through the other polishing stages of 1μm and 0.25μm paste. The final check of orientation was performed using a He-Ne laser (see figure 8). The reflection off the surface gave points lying in a circle, when the jig was aligned along the beam axis and rotated. If the radius was such that the angle subtending it was less than 0.5°, then the crystal was said to be aligned sufficiently for use. The final stage involved mild vibratory polishing using the 0.05μm alumina slurry for about 1 day.

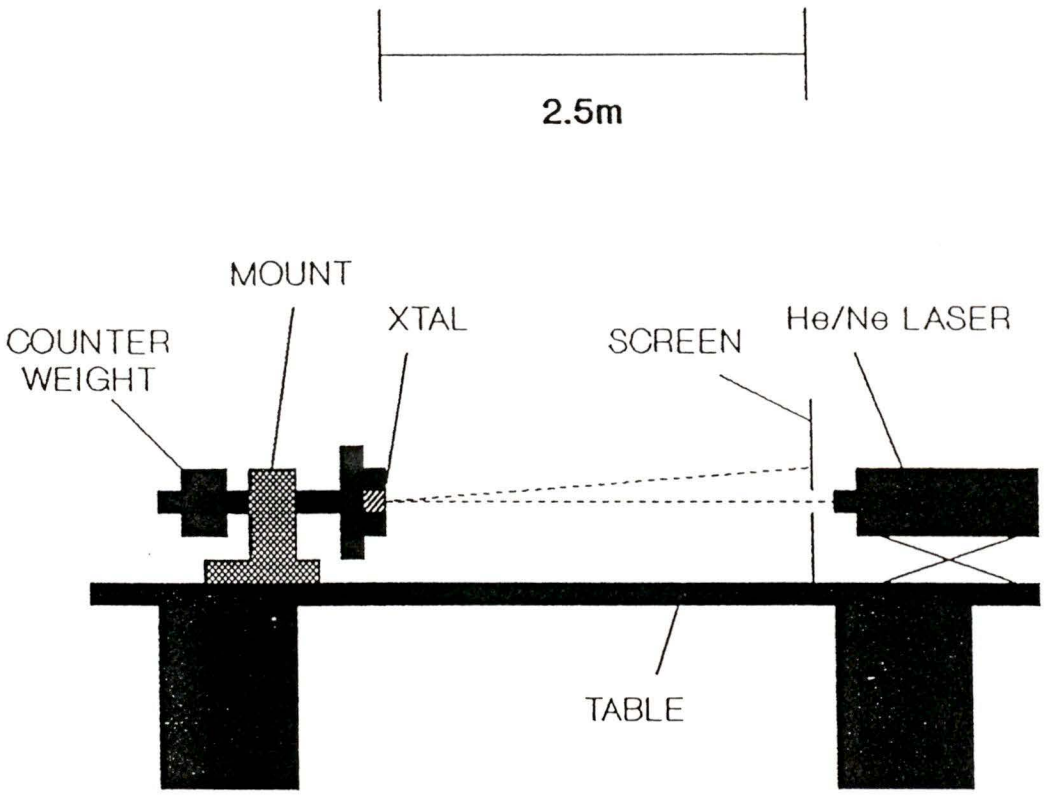

Figure 8: Laser Equipment Configuration Used for Ni(111) Final Orientation Check

2.4 - Reagent Grades Used in Aqueous Experiments.

For all experiments, the purge gases used were H_2 (Union Carbide; oxygen-free ultra-pure grade) and Ar (high purity; moisture-free). The NaOH used in all experiments was ACS grade (BDH), and the H_2SO_4 employed for the electropolishing bath was ACS grade (Fisher). The H_2O used to make up all aqueous solutions was ultrapurified using a Millipore Milli-Q water purification system. The unit employed has two ion-exchange cartridges (Ion-ex*), one activated carbon particle filter (Super-C*), and an organic removal filter (Organex-Q*). The final filter was a microporous 0.22μm Milli-pak* filter which is used to remove micro-organisms

2.5 - Non-aqueous Solvent Handling Procedures.

The acetonitrile (AN) used in these experiments was HPLC grade (Fisher; 99.9+%); with a very low H_2O content (<0.005% w/w). The acetic acid used for an improved polishing bath in the non-aqueous work was 99.7% glacial acetic acid (Canlab).

---

* All filters are a trademark of Millipore Corporation.

The acetic anhydride used to remove trace water from the solution was ACS grade (BDH). The sodium acetate used for the electrolyte was the trihydrate (ACS grade from Aldrich) The following procedures apply to the preparation of the non-aqueous solvent prior to the elution and cycling experiments.

Solvent was poured into a holding bottle, with about 10-20g of anhydrous $MgSO_4$ (Caledon; reagent grade), for drying the solvent. In the solvent, the electrolyte, $NaClO_4 \cdot H_2O$ (BDH reagent grade), was dissolved to give a concentration of 0.3M. The drying agent was employed to remove the water of crystallization from the salt prior to any experiments. The suspension was allowed to settle, and then the solvent was decanted into another bottle with 4Å molecular sieves, and was left overnight in the bottle, sealed with teflon. In some of the earlier exploratory investigations, the 4Å treatment was left out without detrimental results. After drying, the solvent was purged with Ar for 25-40 minutes before transfer into the cell. The dried cell was also purged with Ar for about 20 minutes to help keep H_2O out of the cell before electrolyte transfer. The solution was transferred after the purge step(s), and continued to be purged during the experiments.

2.6 - Electrode Preparation Before Immersion.

The nickel working electrodes were cleaned in the electropolishing solution used for the aqueous studies, as described earlier. For the non-aqueous systems, an aqueous electropolishing solution transfer technique is not very practical, because it is a rather lengthy and difficult procedure to try controlling the amounts of water in the solution during the elution procedure. Instead, the electrode surfaces were immersed in a glacial acetic acid solution (Fisher; 99.5% w/w) for 2 min (without stirring). After immersion, the electrodes were rinsed thoroughly in the appropriate non-aqueous solvent being used. The electrodes were then very rapidly immersed in the electrolyte under potentiostatic control (E held at rather negative potentials (-1.5V vs our reference (see below))). The experiments were then able to be performed using cyclic voltammetry.

2.7 - Reference Electrodes Employed.

The reference electrodes employed in the aqueous work were both hydrogen electrodes, using platinized Pt as the

electrode material. They were fabricated by mounting and sealing a Pt wire in soft glass, then cleaning in acetone and isopropanol. The electrode was then treated with aqua regia (1:1 $HCl:HNO_3$) for 1 minute. It was then rinsed thoroughly with UHP water. The electrode was platinized galvanostatically in a solution of H_2PtCl_6 in 1M HCl, at a current density of $1.3mA/cm^2$, after cycling between the potential limits (O_2 and H_2 evolution regions) once (held in each gas evolution region for 1 minute). The platinization step was carried out for about 10 minutes or until the electrode surface dulled to a blackish-grey, whichever came first. The reference electrode so treated was then removed from the plating solution, and stored in UHP water in a re-sealable test tube. The Pt reference electrode was employed in two distinctly different configurations. The first one (RHE) was as an *in situ* reference, with H_2 used as the purge gas, saturating the electrolyte. The second mode of use was in a sidearm compartment (isolated by a wetted stopcock), as a reference at a known pH. Here, the electrode was inserted into a glass sleeve which had H_2 bubbling in it, and the 1M NaOH electrolyte to be used for the main experiment. This second reference was used often in conjunction with the first one to monitor pH changes in the cell during elution.

The reference electrode used in the non-aqueous work was an Ag/AgCl electrode in acetonitrile (AN), saturated with KCl. The wire electrode was made by cleaning an Ag wire with isopropanol and mounting/sealing in epoxy into a glass tube. The wire was then treated with 50% v/v HNO_3 for 30 seconds, then rinsed with UHP H_2O. Galvanic anodization took place in 1M HCl at $4mA/cm^2$ for 10 minutes. The electrode took on a blackened appearance. The electrode was then rinsed with water again, and left in the solvent saturated with KCl. Liquid junction effects were minimized by employing the same concentration of the $NaClO_4$ electrolyte in the Ag/AgCl reference electrode as was in the solvent.

The potential of the reference electrode was determined at open-circuit versus an *in-situ* RHE reference. The solvent conditions were chosen to ensure that the hydrogen evolution reaction was at equilibrium. 2.0mL of conc. (70%) $HClO_4$ was added to a solution of 0.7mL H_2O in about 400mL of AN. The solution was mixed thoroughly and topped up to a total volume of 500mL ($a_{H^+} = 0.0127m$). The acidic conditions (pH = 1.5) were thought to facilitate and stabilize the H.E.R. in AN. H_2O was present at a molar ratio of *just over* 4:1 with the H^+ ions, this being done to ensure proper solvation of

the H^+ in solution, since H^+ ions are not solvated well in acetonitrile [24].

The measured open-circuit potential was -100mV. A calculation was performed to determine the potential of the RHE (vs the SHE potential scale) in the AN solution. This involved the use of extended Debye-Hückel theory to determine the activity coefficient of H^+ in solution. The assumptions made were that the solvent dielectric constant and density approached that of pure acetonitrile, and the closest approach distance was about 2Å.

The calculated activity values were put into a Nernst expression for the H.E.R. with the potential being adjusted for the free energy changes accompanying transfer of the ions to a non-aqueous medium. The calculated value for the RHE potential was determined to be +390mV. This gave a calculated value of +290mV for the Ag/AgCl reference versus the SHE scale. A check of the calculated value for the reference potential was then carried out. This involved lining up the hydrogen evolution curves between the first voltammograms obtained from the Ni disk experiments carried out in 1M NaOH and in acetonitrile with water added. The two

sets of data were overlaid. The Ag/AgCl reference electrode potential (0.0V) was marked on the voltage scale. The SHE (0.00V) potential was also marked, taking the zero potential for the RHE and adjusting for the pH shift of the H.E.R. in the 1M NaOH solution ($E_{RHE} = E_{SHE} - 0.0592pH$). The potential difference between the SHE and the Ag/AgCl reference electrode was determined to be +304mV. This gives a discrepancy of about 14mV between the empirical measurement and the calculated value of the Ag/AgCl reference potential. This is acceptable, considering the fact that unknown liquid-junction potential contributions are probably present. The low value of 14mV for the discrepancy is considered to be rather good, and suggests that the assumptions made for the solvent system are indeed valid. The reference electrode potential was assigned a value of +297±7mV, which is the average of the two values derived by calculation and experimental methods.

2.8 - Equipment Types Used and their Specifications.

The equipment employed for the cyclic voltammetric studies on the nickel system are shown in figure 9 and were as follows: The potentiostat/galvanostat was a Thompson E401, with modifications for cell isolation using a

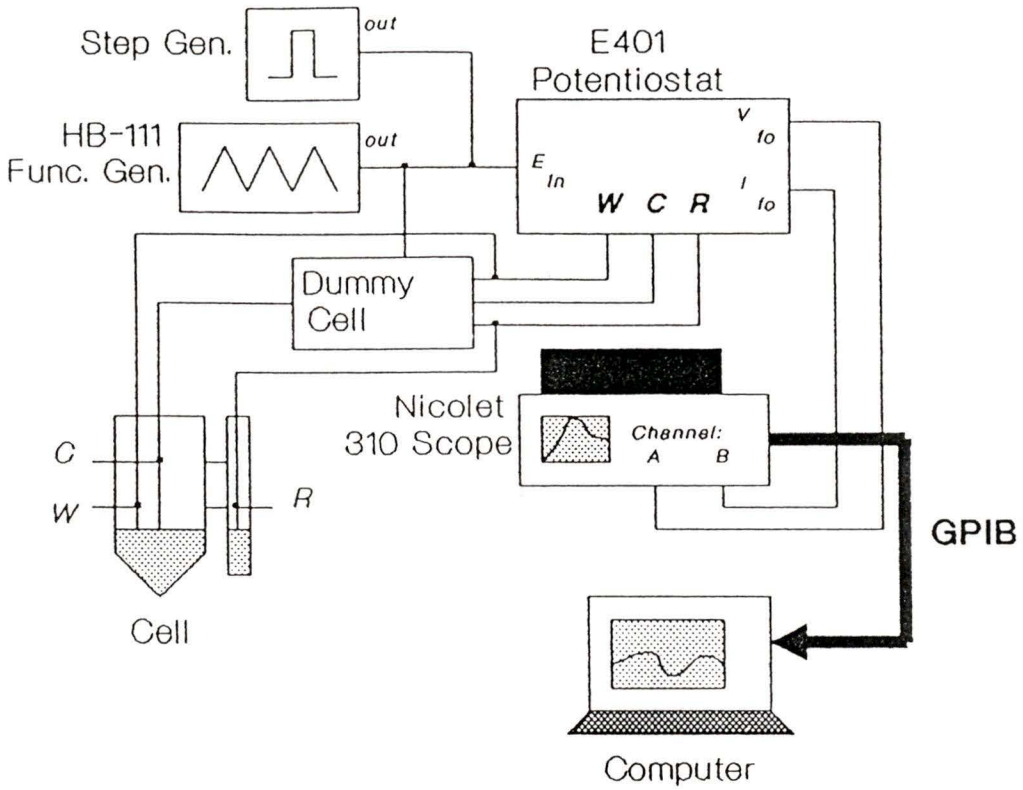

Figure 9: Instrumental Set-up for Elution Experiments
(For detail of Dummy Cell, see figure 15)

pulse-triggered FET switch to control a mercury-wetted relay for opening the circuit. The potentiostat was capable of putting a maximum of about 40V between the working and counter electrodes, and delivering a maximum full current of about 750mA if required. The unit had facilities for extra potential inputs and an external mode input (for switching from potentiostatic to galvanostatic control) incorporated into it. The switching time of the switch for mode conversion was less than 100ns for complete mode switchover. The sweep generator employed was a Hokuto-Denko HB-111 function generator. This was modified to allow triggering of the oscilloscope (Nicolet 310 digital storage oscilloscope) by a pulse from the logic control circuitry in the HB-111. When a potential sweep was initiated, the scope was slaved to the unit and began its traces concurrently with those of the function generator. The generator was also able to do sweep/step and step/sweep voltammetric investigations using the modification just described.

The Nicolet 310 storage oscilloscope was able to follow the progress of each series of cycles by having the voltage and current followers connected directly to it. The scope has differential inputs for measuring floating potentials with either of its two channels. Maximum sensitivity is on

the 100mV scale; the resolution on this setting is to the nearest 50μV. The memory can store 4000 points, and the time base can be set from 1μs to 200s *per* point. Typical time resolution was on the 20ms-50ms per point time range, which allowed from one to about five cycles to be recorded at a time, depending on the potential ranges selected.

A step generator was used for the electropolishing/elution steps in the aqueous work, and its synchronizing pulse facility was employed in switching modes on the E401 potentiostat. This was manufactured in the Chemistry Department's electrical workshop facilities. It is capable of voltage regulation to the nearest 1μV, and can output pulses of up to ±2.00V. The pulse risetime is much faster than the potentiostat's response time.

Discussion of Results

3.1 - Electropolishing Procedure Employed in This Study:

The in-situ elution procedure was the method used in this work to ensure that the nickel surface was at no time exposed to atmospheric oxygen. This technique keeps the surface submerged at all times, and under constant potentiostatic control, preventing inadvertent oxidation of the surface during the switching of solvents in the electrochemical cell.

The surface was first electropolished using an acidic solution consisting of 67% v/v H_2SO_4. This standard electropolishing technique was employed as the first step in smoothing the nickel surface. Electropolishing works by the forced differential dissolution of metal at the electrode surface [25,26]. Because the electric field density at the prominences of the surface is much higher than that seen at the "valleys", metal will dissolve much more rapidly from the peaks, thereby smoothing the surface. The electropolishing procedure also results in the formation of an oxide layer (6-9Å thick) [22] due to the large positive potentials used. The thickness of this layer is determined

by the rate of formation of oxide at the surface as well as the diffusion of dissolved oxide away from the surface in the acidic medium. The layer is necessary for successful polishing, because it aids the removal of metal from the surface. A fairly viscous "Jacquet layer" is formed to a distance of about 1μm from the surface, with a high concentration of dissolved metal cations, as well as a large amount of dissolved metal oxide and oxygen gas. The rate of removal of this Jacquet layer from the surface limits the rate of polishing of the surface.

In initial studies, the electropolishing procedure was employed in the hope that it might further smooth the electrode surfaces under study. Further investigations showed that the electrodes actually roughen with further repeated "polishing". This therefore made the procedure unsuitable for further studies because highly polished electrodes were required, particularly in the case of the Ni(111) single crystal electrode.

3.2 - Elution Procedure.

The polishing and elution procedure developed here had several steps to ensure that the electrode surface was in an oxide-free state prior to cycling experiments. The first of these involved an electropolishing step, as described above. The solution used for electropolishing initially was 67% v/v H_2SO_4 (2:1 by volume with H_2O). This solution was purged with hydrogen for at least 30 minutes before use. The electrode was electropolished for 2 minutes at an optimal current density of $0.4A/cm^2$. During such a polishing step, oxygen gas was observed to be generated quite vigorously at the working electrode.

The electropolishing step was followed by an open circuit isolation of the cell for about 4 minutes. The layers of oxide dissolve in the acidic polishing solution during this time. Eventually, all the oxide is removed and then bare metal begins to slowly dissolve in the solution, with the evolution of some H_2 gas. During the removal of oxide from the metal, the potential of the working electrode shifted to less positive values, and a flattening of the potential versus time curve was observed. The electrode eventually reached a steady-state condition where it is thought that

the oxide is removed and only bulk metal is dissolving slowly. This behavior of the system is seen in figure 10. The desired oxide-free surface condition of the electrode is believed to have been achieved by the above treatment.

After the open circuit isolation step, the cell was then re-engaged potentiostatically at -0.3V vs an RHE reference electrode, situated in the main part of the cell (see figure 11). Hydrogen gas evolution was evident from the bubbles observed emanating from the electrode. The cell was then simultaneously filled with the 1.0M NaOH eluent (this was previously purged with hydrogen before the experiment) while draining the polishing solution (H_2SO_4); both of these were done at a flow rate of approximately 1.2mL/s. The total cell volume was about 40mL.

A simple model was used to describe the mixing (figure 12). The assumptions for it are that solution mixing is very fast compared to the flow rates, and that the cell volume does not change during the elution (i.e. the inflow and outflow rates are equal). These assumptions are only approximately adhered to, but are adequate for first-order estimates. The differential equation describing the system's dynamics under these conditions is also given in the

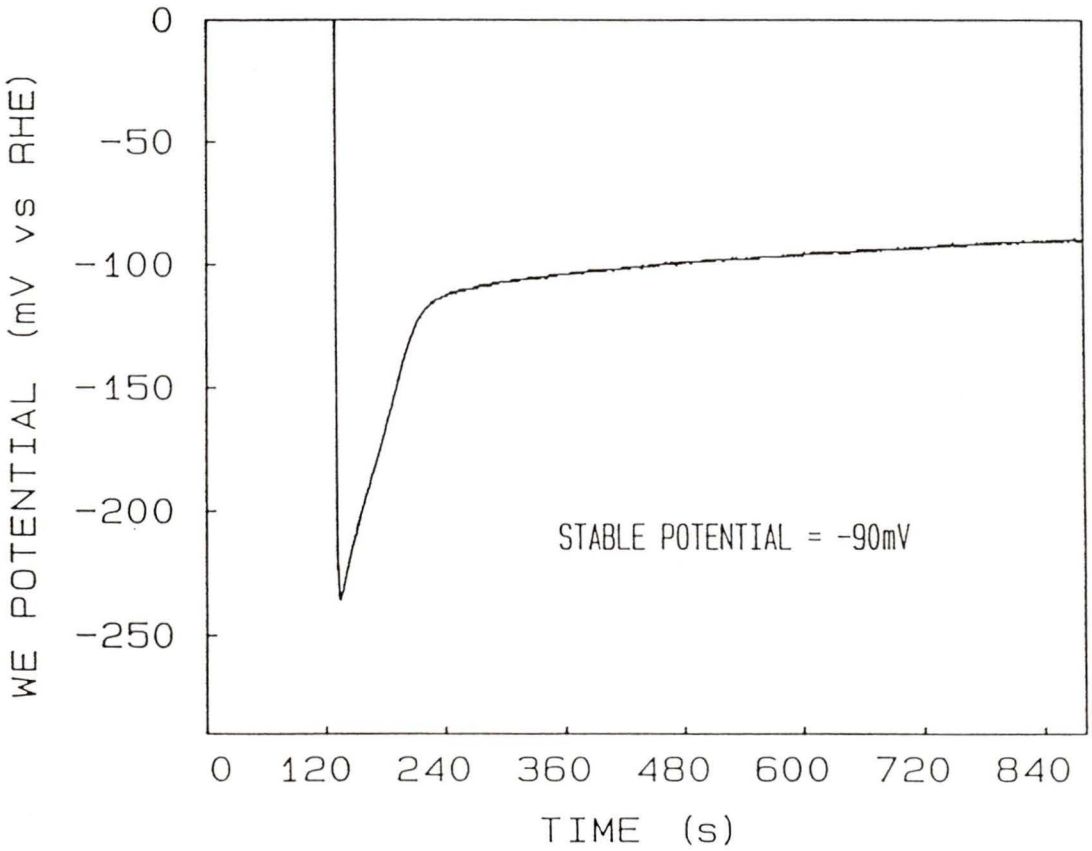

Figure 10: Open Circuit Potential Behavior with Time upon Isolation of the Cell

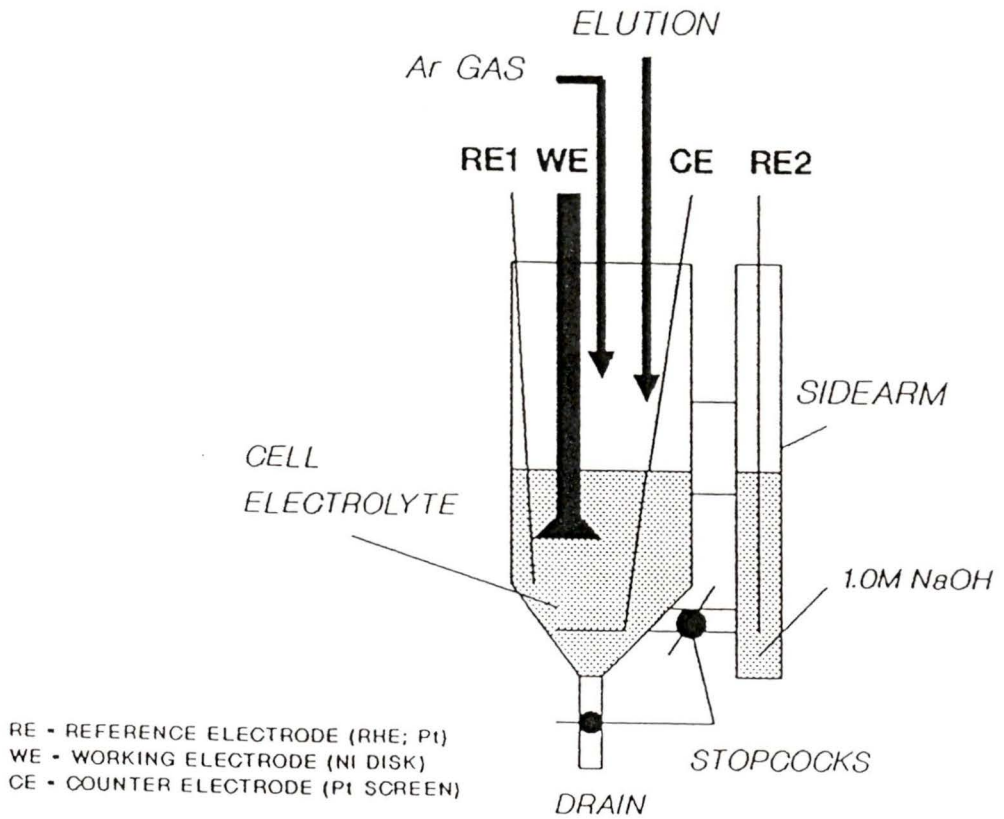

Figure 11: Electrode Configuration in the Elution Cell

equations in figure 12. dA'/dt is the change in concentration of the electrolyte in the cell. dV'/dt is the flow rate into (and out of) the cell. A is the bulk concentration of eluent. The solution of this differential equation leads to equation (1).

The equation describing the concentration of the solution in the cell as a function of elution time was developed to predict the time required for essentially complete solution exchange:

$$A' = A (1 - \exp(-C_f t/V)) \quad (1)$$

Where C_f is the flow rate (in mL/s) of the solutions, A is the concentration of the NaOH solution (1.0M), V is the volume of the cell, t is the elapsed elution time, and A' is the concentration of the eluent at time t. This equation can be rearranged to yield the following expression:

$$t = (-V/C_f) \ln (1 - A'/A) \quad (2)$$

Using the above values in the expression, gives a value of t of 230.3s, or about 3.84 minutes to convert the electrolyte to 99.9% of the bulk concentration of the NaOH (1M).

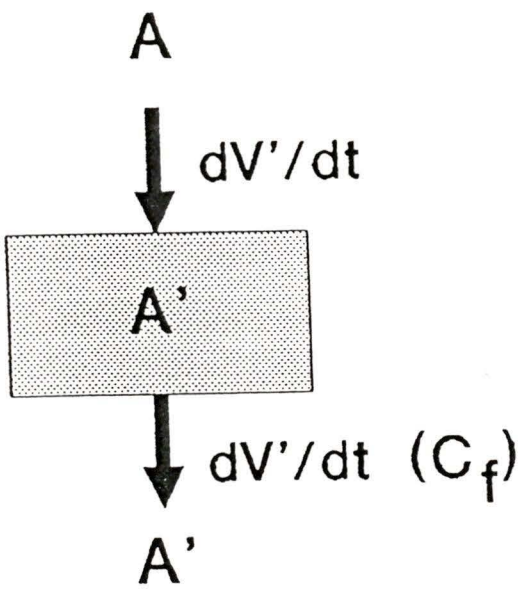

$$V \frac{dA'}{dt} = A \frac{dV'}{dt} - A' \frac{dV'}{dt}$$

$$A' = A\,(1-\exp(-C_f t/V))$$

Figure 12: Flow Dynamics Model for the Elution Experiments

During the elution, one expects to see changes in pH with time, because the solution is changing over from an acidic one to the alkaline 1.0M NaOH. This is indeed observed as the elution progresses. The pH of the system during elution was monitored by utilizing a second reference electrode external to the cell. This reference electrode was also a hydrogen electrode, but it was always kept in a 1.0M NaOH solution. The potential difference between this reference electrode and the internal RHE is 59mV per pH unit. The NaOH eluent is at a pH of 14 and can be used to find the absolute pH of the solution in the cell if desired. When the potential difference between the two reference electrodes is very close to zero, the elution is complete and the electrolyte is 1M NaOH. Since the elution takes about 4 minutes to complete, the dynamical model and equation describing the elution behavior are in agreement and are considered to adequately describe the elution. The main difference is probably in the assumption that there is virtually instantaneous mixing of solutions. During the elution, the pH curve is observed to have two rapid changes which look surprisingly like a titration curve. This curve can be seen in figure 13. This behavior can be explained as a neutralization of the solution during the elution run. Since H_2SO_4 has two removable protons, it is expected that

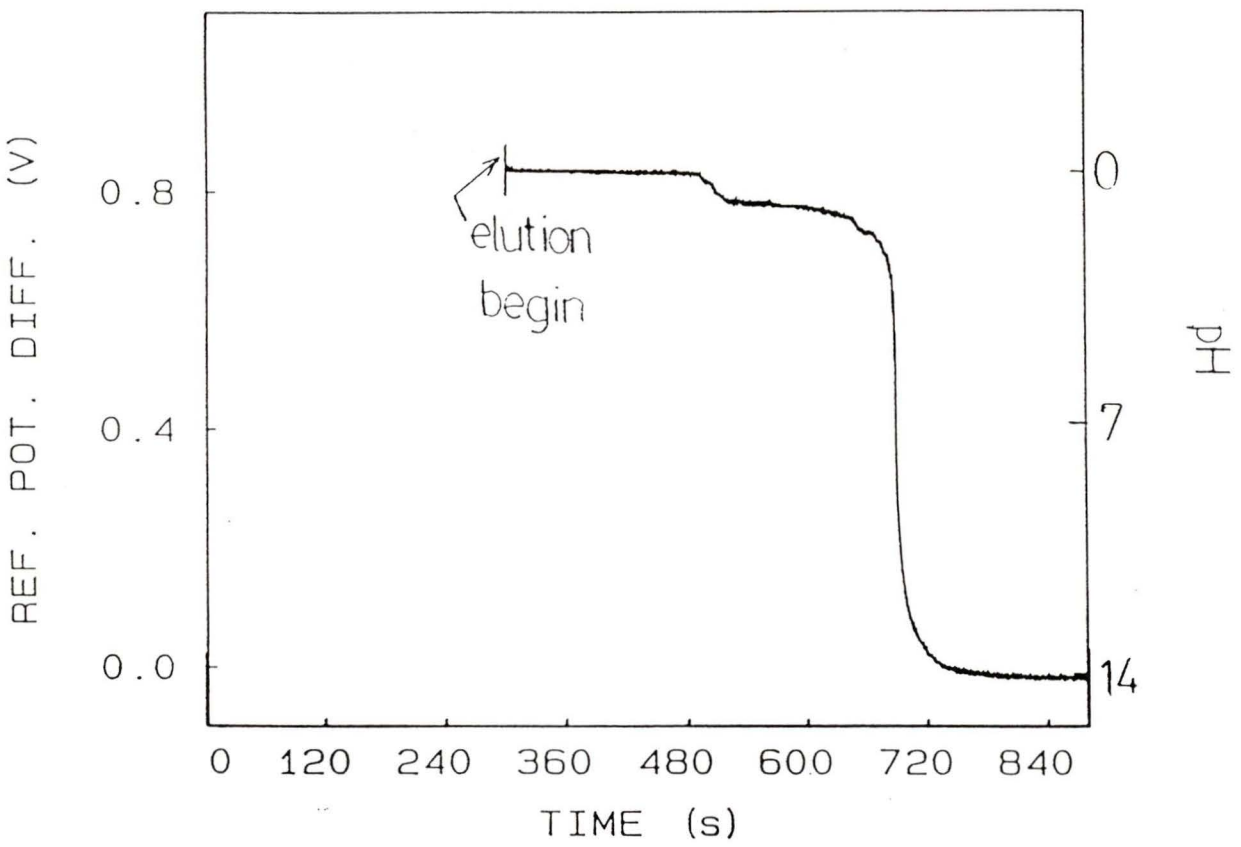

Figure 13: Reference Electrode Behavior and pH Changes in the Cell During a Typical Elution Experiment

there should be two points during the elution when the electrolyte species has a proton removed by the alkaline eluent (OH^-). The pK_a for each proton is different, with one proton coming off quite easily leaving HSO_4^- ions in solution. When the last proton off the sulphate moiety has been removed, the solution is at the same pH obtained by dissolving Na_2SO_4 in water. Further addition of eluent to the cell causes the pH of the system to rapidly approach 14 as the $[OH^-]$ increases. This is observed as a potential difference of zero between the reference electrodes, as mentioned earlier.

The elution itself was performed potentiostatically versus the internal RHE reference electrode. The potential of this electrode changes with pH, as does the potential of the hydrogen evolution reaction at the nickel electrode. As the elution progresses, the working electrode (Ni) is held at -0.3V vs RHE (internal), while the potentials of both electrodes become gradually more cathodic versus the external hydrogen reference electrode in 1.0M NaOH. At the end of a typical elution run, the working electrode was generating small amounts of hydrogen with the potential difference between the two reference electrodes being a few millivolts: the working electrode is now in 1M NaOH.

The current flowing in the system was also monitored during the elution (see figure 14). It was observed to dip to large cathodic values during most of the elution. The total charge passed during elution was about $-9.8 C/cm^2$. The amount of charge required to reduce any oxide on the surface would be several orders of magnitude lower, even for 10 oxide layers. Therefore, the observed charge was assumed to be due to hydrogen evolution. Near the end of the elution, the current rose to *less cathodic* values, so that no net oxidation was occuring. Thus, the procedure yields an electrode surface which is likely both clean and oxide-free, since oxides cannot form at the potential at which the electrode was held. The electrode was then ready for study using cyclic voltammetry.

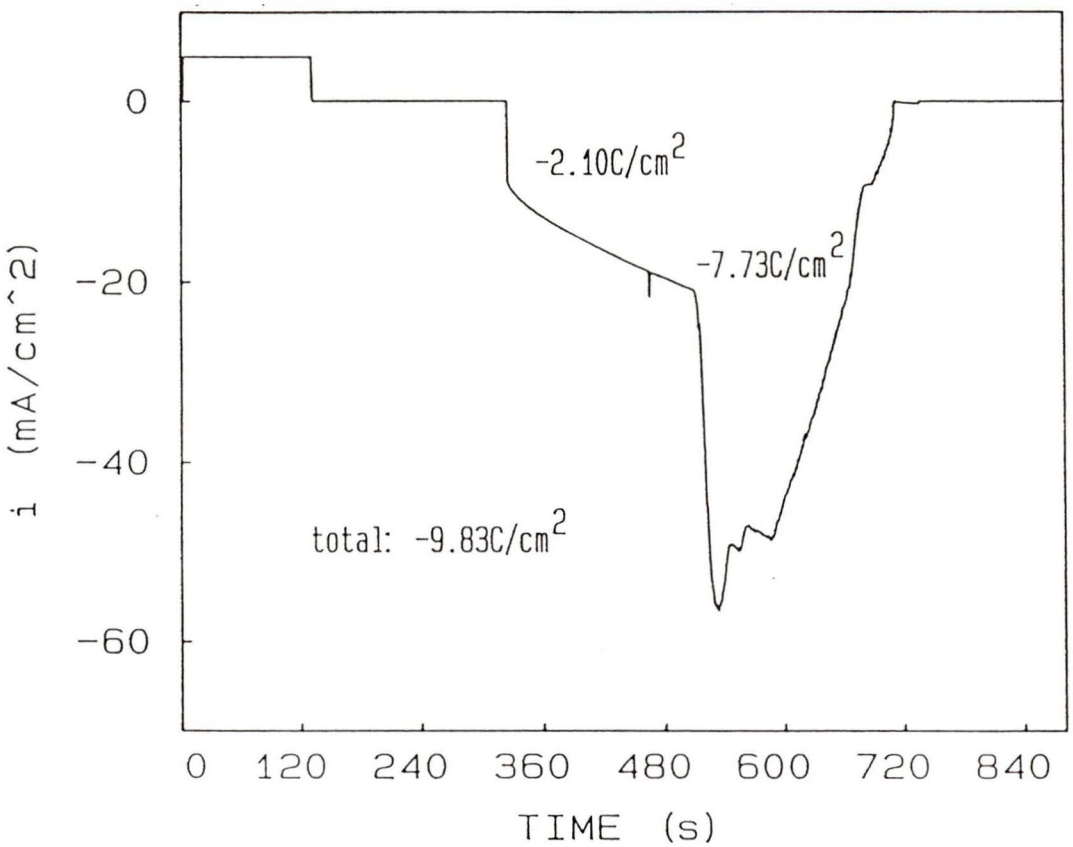

Figure 14: Current Behavior During a Typical Elution

3.3 - Elution Problems and Solutions.

Initially, the entire elution procedure was to be carried out while reducing in galvanostatic mode. Unfortunately, the potential of the working electrode was observed to be sufficiently positive to allow oxide formation. The potentiostatic approach was therefore employed instead to avoid any further problems with assuring an oxide-free electrode.

Some problems with the elution procedure were observed that were unforeseen prior to the development of this technique. The first was the apparent roughening of the polycrystalline wire samples with repeated use. In these preliminary experiments, the electrode surface gradually became pitted and etched, clearly indicating that the electropolishing step was steadily degrading the quality of the surface finish. This may have been primarily due to the poor electrode geometry in the cell. If the electrode configurations employed were not optimally set up, there remained the possibility that there would be non-uniform electric field gradients at the surface of the electrode, leading to some areas having current densities in the "pit" or "etch" regions. This was obviously the case, and led to

the observed results. The best solution to this was to avoid an electrochemical polishing step totally, to avoid degrading the more highly finished and easily damaged Ni(111) electrode used in later experiments. As a consequence, a chemical polishing bath comprising 0.3M sodium acetate in 100% acetic acid (with an excess of acetic anhydride) was used to remove the oxide from the surface. In order to validate this procedure, solubility tests for Ni, NiO, and $Ni(OH)_2$ in the bath were performed, with interesting results. The oxide and hydroxide were readily soluble in the solution, as indicated by the green tint in the resulting solutions, characteristic of Ni^{2+}. Ni metal was not extensively attacked by the solution. This was optimal, since a highly finished electrode surface with an oxide coating would have the oxide removed by the solution, *without* extensive loss of metal from the surface prior to elution. The reason the 100% acetic acid was employed was to maintain continuity between the aqueous studies performed and later studies performed with dry acetonitrile (AN) as a solvent. The bath can be used in both systems, and must be free of moisture to keep water levels to a minimum in the AN elutions. The modified elution procedure eliminated the electropolishing step in favor of an open-circuit run in the new bath. When the potential was stable, the elutions were

then carried out.

Another problem with the elution procedure was in the re-engaging of the cell after leaving the system at open circuit. Large potential and current transients occurred during switching to the potential required for elution. Even though the times for these transients were small (about 2.7ms), the potential went to near the maximum obtainable from the amplifier (40V). The potentiostat was for a brief time at an open control loop condition, which caused the unit to go to its "saturation" mode of operation, which happened to be at 40V. In the time during the transient, the charge passed for the transition was about 540μC when using a 200Ω test cell. This amount of charge could possibly result in the formation of about one layer of oxide. This was clearly undesirable, and the first approach to allieviate the problem was to employ ultra-fast FET transistor switching to re-engage the cell. This met with little success, because even though the switching time was reduced to only 70μs, the cell still had the full 40V applied to it during that time, which would result in extensive oxidation of the surface. The problem was solved by employing a dummy cell in parallel with the electrochemical system being studied, switched with a rotary

"make-before-break" switch. The dummy cell is balanced to minimize the transients that would be seen if it were the real cell, and is engaged first. The dummy cell then absorbs the transients without any current being passed to the real cell, since it is still isolated at this point. The real cell is then engaged. The dummy cell's "reference" electrode is read by the E401 potentiostat potential input(s). This completes the control loop of the internal amplifier, thus forcing the unit to retain control and minimize the magnitude of the transients when the real electrochemical cell is engaged. The result of this procedure is to avoid the extensive damage to the surface caused by the large transients. Some small transients still appear, but the total charge passed during cell switchover is reduced to 0.5-2.0$\mu C/cm^2$, less than 1% of the total charge required to oxidize one layer of nickel on the surface. This is acceptable, since it leaves the rest of the surface oxide-free and clean, ready for study. A diagram of the layout of the dummy cell can be seen in figure 15.

3.4 - Acetonitrile Elutions.

The same type of elution procedure was applied for the experiments performed in acetonitrile (AN). The solutions

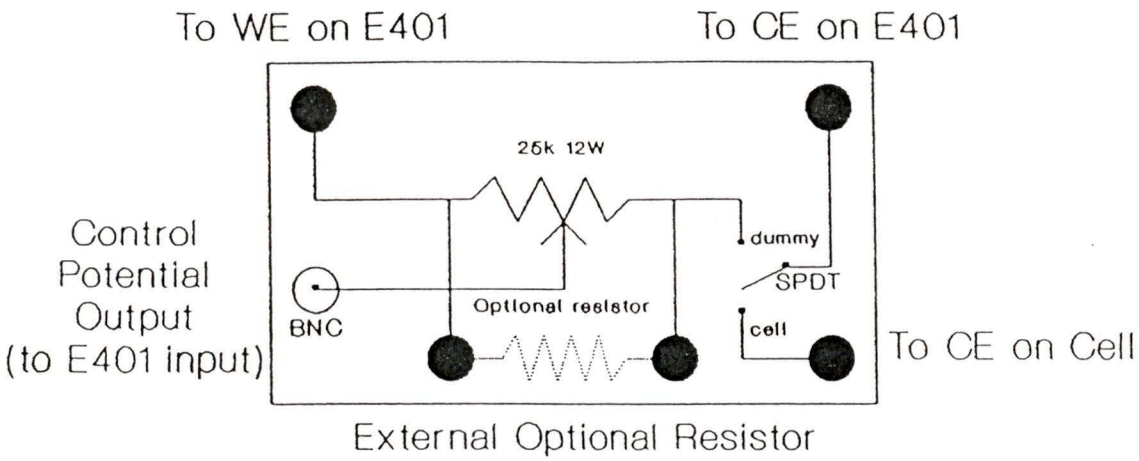

Figure 15: Dummy Cell Configuration

had to be as free from water as possible, and the 100% acetic acid polishing bath was required for these experiments. The electrode (rotating disk: f_{Rot} = 33Hz, d = 0.5cm) was left at open circuit for about 2 minutes, or as long as it took to achieve a steady-state potential. The cell was then re-engaged using the switching arrangement described above. Elution followed, with the potential of the electrode being maintained at -1.6V versus a Ag/AgCl reference electrode in AN with 0.3M $NaClO_4$. The electrolyte used for the AN eluent was 0.3M $NaClO_4$ (the electrolyte in the reference was the same to minimize any liquid-junction contributions to the potential difference in the system). The current was large and cathodic during the elution, indicating that the electrode was maintained in a reduced state thoughout the elution.

The end of the elution was usually signalled by a cathodic current paralleling the behavior seen in the aqueous systems studied. The electrode was again left in an oxide-free, reduced condition, ready for the cycling experiments to be performed.

3.5 - Rotating Disk Study in Aqueous Solution.

Experimental results from the study of the polycrystalline disk electrode showed promising results. The electrode was polished to a 6μm finish, as described earlier. The surface integrity, with regards to its macroscopic mirror-like appearance, was maintained throughout all experimental elution runs. At no time did the surface lose its finish, or become irreversibly coated with a visible film. This was the situation hoped for when the change of polishing solution was carried out for these experiments. The disk was rotated throughout the elution and voltammetry experiments at a rate of about 200rpm (33Hz). This rate of rotation was enough to remove any gas bubbles from the surface due to either gas evolution at the electrode, or the purge gas present in the cell.

3.6 - Results for the Polycrystalline Disk Electrode in 1.0M NaOH.

In all investigations in aqueous solution, cyclic voltammetry was carried out after the elution was complete. The sweep rate was 100mV/s and the potential at the start of cycling was -0.3V vs RHE. The upper range was initially 0.0V for three cycles, then this was extended to +0.8V for three more cycles. The upper potential limit was then extended during continuous cycling of the electrode potential to +1.5V for about three further cycles. The sequence of extending the range was then reversed while still cycling, such that the limit was reduced to +0.8V once again for three cycles, then to +0.0V. The fourth cycle on the last stage was extended back to +1.5V. This sequence was used to investigate the difference in the behavior of the electrode depending on the potential range. The electrode was rotated at about 200rpm (f = 33Hz) during all experiments to remove hydrogen gas bubbles which otherwise have a tendency to stick to the electrode surface. The potentials for the major peaks in the cyclic voltammograms can be seen in Table 2.

Table 2: Observed Peak Potentials for the Aqueous Systems

Ni Disk in 1M NaOH: Elution Procedure Surface Preparation	
Peak Designation:	Potential (vs RHE; pH = 14)
α': Ni $\longrightarrow$ Ni^{2+}	+0.170V
α : Ni $\longrightarrow$ α-$Ni(OH)_2$	+0.317V
γ_r: γ-NiOOH $\longrightarrow$ α-$Ni(OH)_2$	+1.332V
Ni Disk in 1M NaOH: MacDougall Procedure Surface Prep.	
Peak Designation:	Potential (vs RHE; pH = 14)
α': Ni $\longrightarrow$ Ni^{2+}	+0.142V
α : Ni $\longrightarrow$ α-$Ni(OH)_2$	+0.338V
γ_r: γ-NiOOH $\longrightarrow$ α-$Ni(OH)_2$	+1.306V
Ni(111) in 1M NaOH: Elution Procedure Surface Preparation	
α': Ni $\longrightarrow$ Ni^{2+}	+0.165V
α : Ni $\longrightarrow$ α-$Ni(OH)_2$	+0.347V
β_o: β-$Ni(OH)_2$ $\longrightarrow$ β-NiOOH	+1.22V (est.)
γ_r: γ-NiOOH $\longrightarrow$ α-$Ni(OH)_2$	+1.338V
β_r: β-NiOOH $\longrightarrow$ β-$Ni(OH)_2$	+1.298V

NOTE:

The subscripts "o" and "r" denote peaks for oxidation and reduction processes respectively. (e.g. γ_r is the peak attributed to the reduction of γ-NiOOH.)

3.6.1 - Elution Procedure Behavior of the Nickel Rotating Disk Electrode.

The behavior during elution for the nickel rotating disk electrode was as expected in all experiments. The electrode remained in a reduced condition throughout the elution, as evidenced by the large cathodic current observed. In the aqueous studies of the nickel disk electrode to be described, the eluent was 1.0M NaOH.

3.6.2 - Cyclic Voltammetry Results for Nickel Disk Prepared via the Elution Procedure.

Beginning with the surface prepared by the elution procedure, cycling to about 0.0V (cycles 1-3 of figure 16) showed a small amount of oxidation to the α-hydroxide and subsequent reduction back to the metal. The process evidently leads to no net change in the surface structure, since oxidation and reduction charges are approximately equal (see table 3), and subsequent cycles overlap. The charge densities were calculated by integrating the current traces in the area of the peaks and dividing by the geometric area of the electrode surface. The reduction current density for each cycle was obtained by integrating

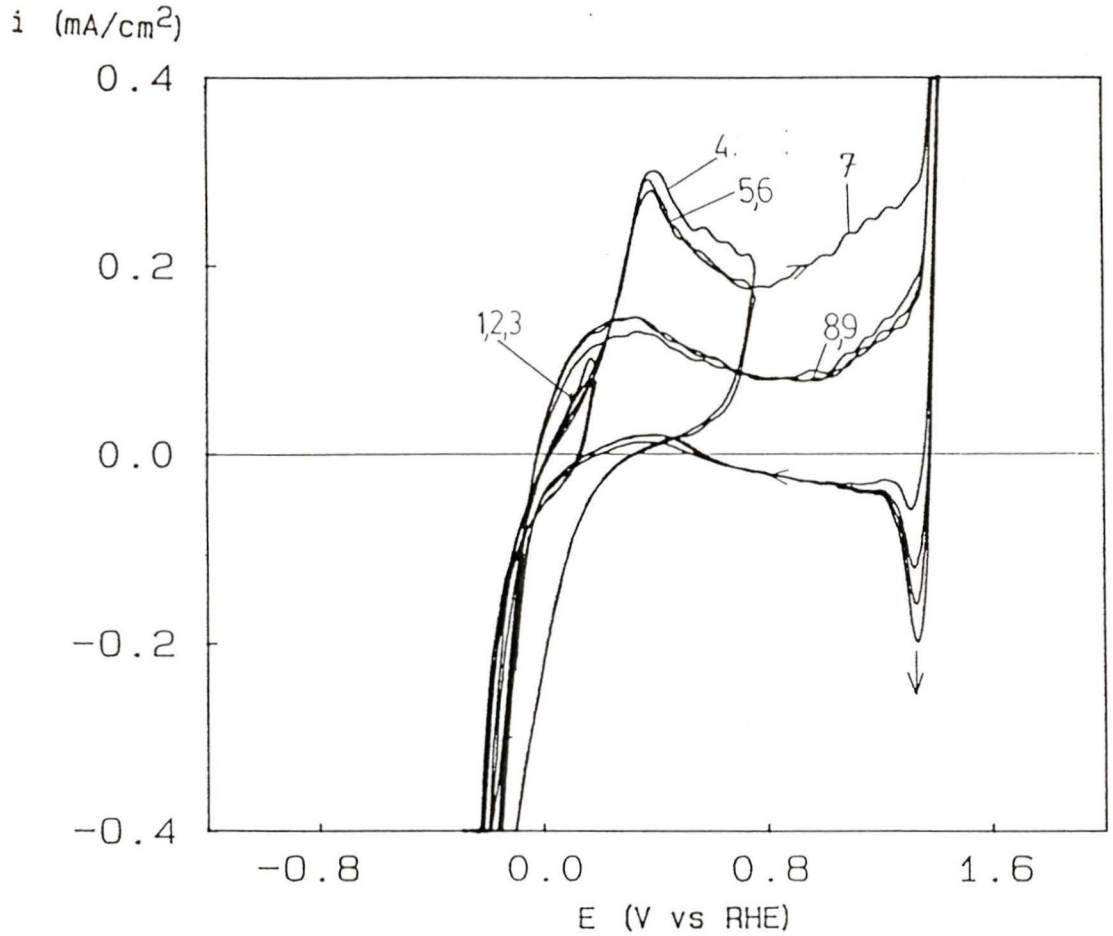

Figure 16: Cyclic Voltammogram (First Cycles) of Nickel Disk Electrode Prepared by the Elution Procedure (in 1M NaOH)

Table 3: Charge Density Data for the Aqueous Systems

Ni (1M NaOH [elution]	Q_a (mC/cm^2)	Q_c (mC/cm^2)	ΔQ (mC/cm^2)	Net oxide coverage, monolayers
cycle: 4	2.26	2.02	0.24	0.42
5	2.06	2.49	-0.43	-0.78
6	2.05	2.50	-0.45	-0.81
7	4.43	1.76	2.68	4.82
8	2.60	1.91	0.70	1.26
9	2.65	1.88	0.78	1.40
12	2.03	1.86	0.17	0.31
16	3.78	1.45	2.32	4.17
17	3.07	2.04	1.03	1.85
Ni (1M NaOH [MacDougall]	Q_a (mC/cm^2)	Q_c (mC/cm^2)	ΔQ (mC/cm^2)	Net oxide coverage, monolayers
cycle: 4	2.27	3.09	-0.82	-1.47
5	2.16	3.11	-0.95	-1.71
6	2.14	2.88	-0.74	-1.33
7	5.75	3.83	1.92	3.45
8	4.75	4.23	0.52	0.93
10	1.76	2.63	-0.87	1.56
17	5.21	4.57	0.64	1.15
18	4.87	4.96	-0.09	0.16
Ni(111) in 1M NaOH [Elution]	Q_a (mC/cm^2)	Q_c (mC/cm^2)	ΔQ (mC/cm^2)	Net oxide coverage, monolayers
cycle: 1	3.16	2.90	0.26	0.45
2	3.08	2.44	0.64	1.07
3	7.32	1.90	5.42	9.09
4	4.15	1.89	2.26	3.79
6	1.93	1.20	0.73	1.22
11	5.03	1.60	3.43	5.76
12	4.47	1.84	2.63	4.41
Ni(111) in 1M NaOH [Beden]	Q_a (mC/cm^2)	Q_c (mC/cm^2)	ΔQ (mC/cm^2)	Net oxide coverage, monolayers
cycle: 1	0.63	0.75	-0.12	0.20
2	0.62	0.66	-0.04	0.07

Note: Q_a and Q_c are the anodic and cathodic charge densities for the cycles shown.

the *total* cathodic charge density and subtracting the contribution due to hydrogen evolution. The disk had an area of 0.198cm^2, while the Ni(111) electrode had an area of 0.785cm^2. In table 3, the value for the calculated amount of oxide on the surface was determined by dividing the charge density determined per cycle by the charge density per monolayer of film. For a (111) surface, the unit mesh charge density is 596μC/cm^2 per layer of oxide. The polycrystalline value of the unit mesh charge density is taken as 556μC/cm^2, which is a value obtained assuming a surface site distribution of 50% coverage by (111) sites and 50% coverage by (100) sites.

Extending the cycles to an upper limit of about 0.8V (vs RHE), gave a complete α-OH peak (cycles 4-6), and showed a decrease in the α-hydroxide peak current density for cycles after cycle 4. The data for the charge passed in the first few cycles is shown in Table 3. The decrease in charge density on successive cycles can be explained as a small loss of reactivity of the electrode surface for oxidation of the nickel atoms to the α-hydroxide. This can be attributed to some conversion of the α-hydroxide to the inactive (i.e. non-reducable) β form. The α peak reduction charges are less than the corresponding oxidation charges (table 3). This may

be an apparent rather than real effect, since additional reduction would be masked by the hydrogen evolution current. On extending the cycling range to +1.5V, the first extended cycle (7 in figure 16) showed considerable oxidation ($4.43 mC/cm^2$) of the surface to the β and γ-oxyhydroxides. Subsequent cycles in this extended potential range showed much less charge, i.e. the first cycle led to considerable passivation of the metal surface. The potential region between 0.8V and the β-OH to γ -OOH peak at about 1.4V is attributed to formation of the β-hydroxide. The reason for the passivation (cycles 8 and 9) is that the β-OH is not reducable, and it inhibits subsequent oxidation. The extension of the range in cycles 7-9 also lead to a marked change in the shape of the α peak, with appearance of a new component, α', as a shoulder on the leading edge. (The two features α and α' are not well resolved in figure 16, but may be seen more clearly elsewhere, e.g. figure 22) This peak has been attributed to either the oxidation of adsorbed surface hydrogen [2], or loss of metallic nickel from the surface, to give Ni^{2+}. Sandoval, Schreibler and Gomez [25] suggest (with their rotating disk work on nickel in 1.0M NaOH) that the cause for the shoulder might be the latter process. The higher their rotation speed, the larger the shoulder becomes until it actually appears as a peak. The

higher rotational speed will increase the rate of removal of Ni^{2+} ions from the disk's surface, thereby allowing a greater number of ions to be removed from the surface during the sweep time in that potential region. However, adsorbed hydrogen on the surface can also be removed as H_2 gas with higher rotation rates of the electrode. Further work in this area may shed some light as to which is the dominant process responsible for the extra "peak" in the α-hydroxide region.

A gradual increase in the β and γ-oxyhydroxide reduction peaks was also observed on extended cycling (cycle 7 on, figure 16). The larger the amount of reducable oxide on the surface, the larger this peak is expected to be. If the charges passed per cycle are integrated, the apparent net result is that the surface is slowly and gradually being oxidized. Since the electrode does not appear to lose activity, it may be that all oxides are reducable, but the additional reduction charge is masked by the H.E.R. This is behavior typical for a nickel electrode in 1.0M NaOH when subjected to continued potential cycling in the "full" range of the solvent. The location of the β and γ-OOH peaks in the most anodic region of the voltammograms was consistent with earlier Ni studies in the literature [1,2,16].

The main feature *not* seen in any of the previous literature experiments with polycrystalline nickel electrodes is the presence of an "anodic excursion" on the negative-going sweep immediately following the β-oxyhydroxide reduction peak. It is possible that on the return sweep, the surface film is reduced sufficiently to expose some bare electrode surface. At the potential where this occurs, oxidation of the exposed metal surface atoms to the α-hydroxide would occur, causing a net oxidation current to be observed. The surface appears to return to the condition that it had prior to cycling into the full potential range, as evidenced by the curve shapes of cycles 16-18 meeting and following cycles 10-12 of figure 17. This behavior warrants further investigation. Cycle 12 shows 90% of the α-OH charge in cycle 4, i.e: the surface appears to regain *almost* all of its surface reactivity when subjected once more to a restricted potential region for a few cycles before cycling once again in the full potential regime. However, the shape of the α peak is different, with a more pronounced α′ state. It appears that a majority of the surface that was oxidized can be reversibly reduced back to nickel, as was seen in the return sweeps mentioned previously.

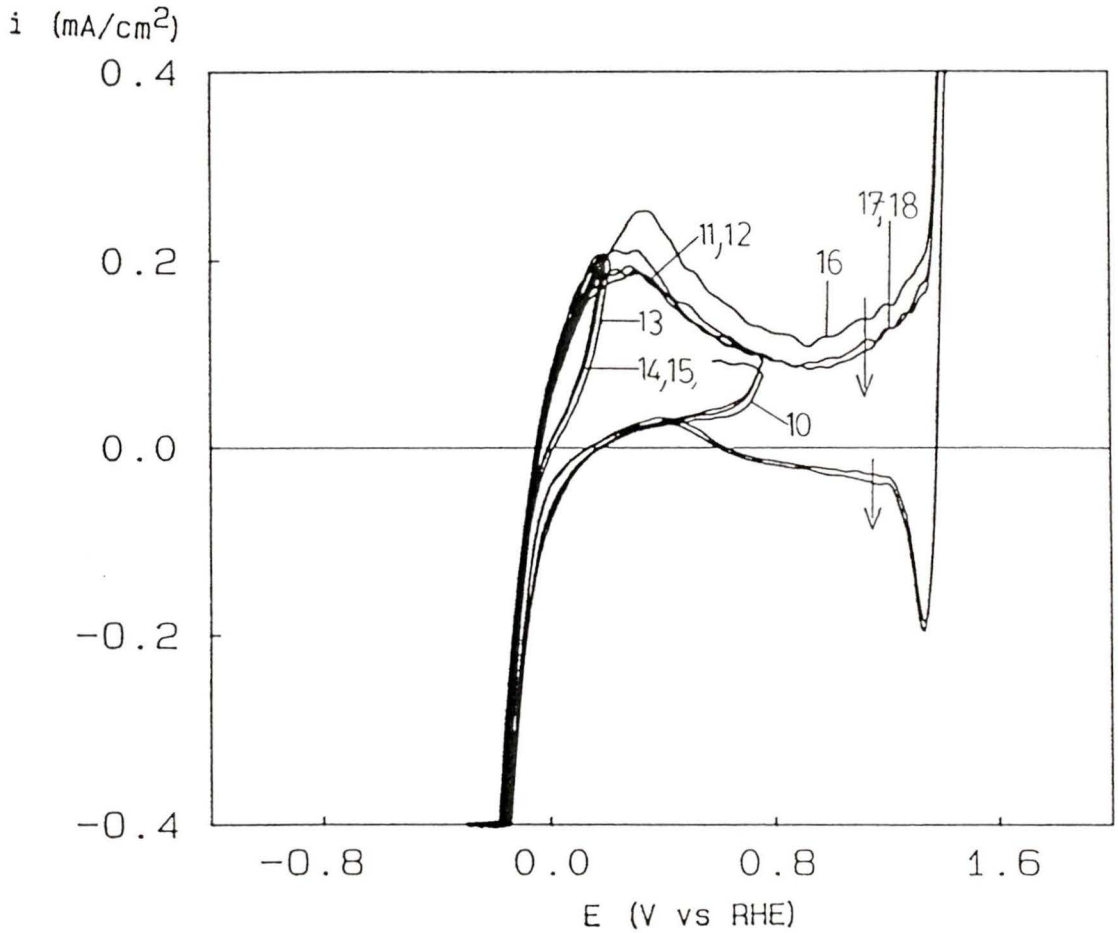

Figure 17: Cycles 10-18 of the Nickel Disk Electrode in 1M NaOH (Elution Procedure)

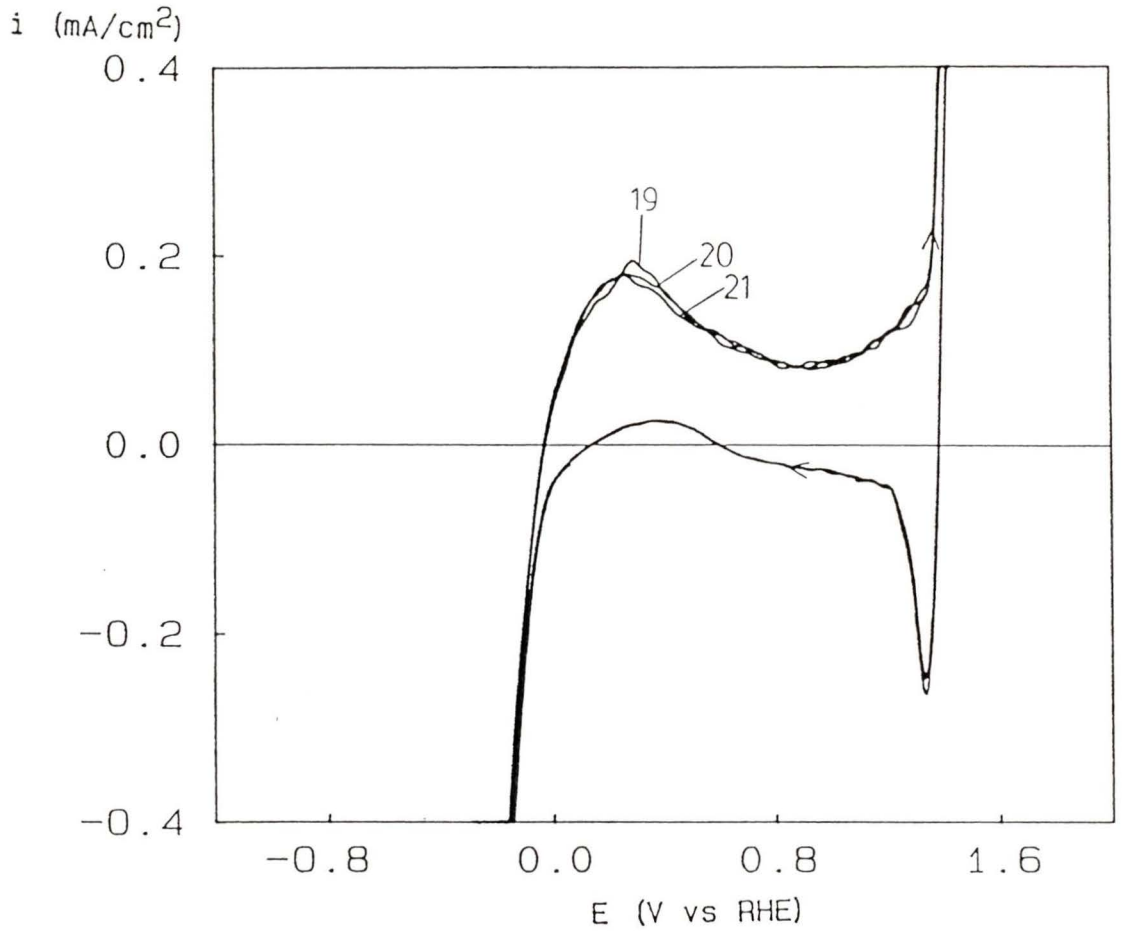

Figure 18: Cycles 19-21 of the Nickel Disk Electrode in 1M NaOH (Elution Procedure)

3.6.3 - Cyclic Voltammetry Results for Experiments with the Nickel disk Prepared by MacDougall's Method.

A literature surface preparation for nickel (MacDougall [22,27]) was also performed on the polycrystalline disk electrode, with interesting results. The preparation involved chemically polishing the nickel electrode in a mixture of 10% H_2SO_4, 10% H_3PO_4, 30% HNO_3, and 50% glacial acetic acid for 30 seconds. The electrode was then electropolished for 2 minutes at a current density of $0.5A/cm^2$. The sample is normally subjected to vacuum annealing at 800^oC and re-electropolishing prior to the performance of experiments on the electrode, but unfortunately our laboratory facilities were not sufficiently equipped at the time of these investigations, and only the electropolishing step was carried out. The annealing step should only aid in further smoothing of the surface. After the chemical polishing step, it was observed that the 6μm surface finish of the electrode was destroyed, and the electrode took on an etched appearance. Thus, electropolishing *did not* sufficiently restore the previous 6μm finish.

As can be seen in figures 19 and 20, cycling behavior was quite similar to that seen in the investigations of nickel using the elution procedure, and the α-hydroxide peak charge densities were also similar. Referring to the table of charge densities passed per cycle (Table 3), it can also be seen that the electrode treated with the elution procedure shows a lower degree of reversible oxidation (as measured by the net difference between oxidation and reduction charges) than does the electrode prepared by MacDougall's preparation, suggesting that a higher proportion of the hydroxide is in the β form. This can be interpreted in the following manner: Because the surface prepared by the elution technique is smoother (judged by the macroscopic appearance of the surface), it may form an α-hydroxide with fewer defects. The film formed is thus inherently more highly crystalline than that formed on the MacDougall electrode, and can convert more readily to the crystalline β form. It is these areas of β-hydroxide that do not get reduced on cycling in the restricted α-hydroxide range. On the MacDougall electrode, the rougher surface forms a more highly disordered α- hydroxide film, which is more easily reducable back to nickel metal and takes longer to transform into the ordered β-phase on the timescale of the cycling experiment. This accounts for the greater net reduction of

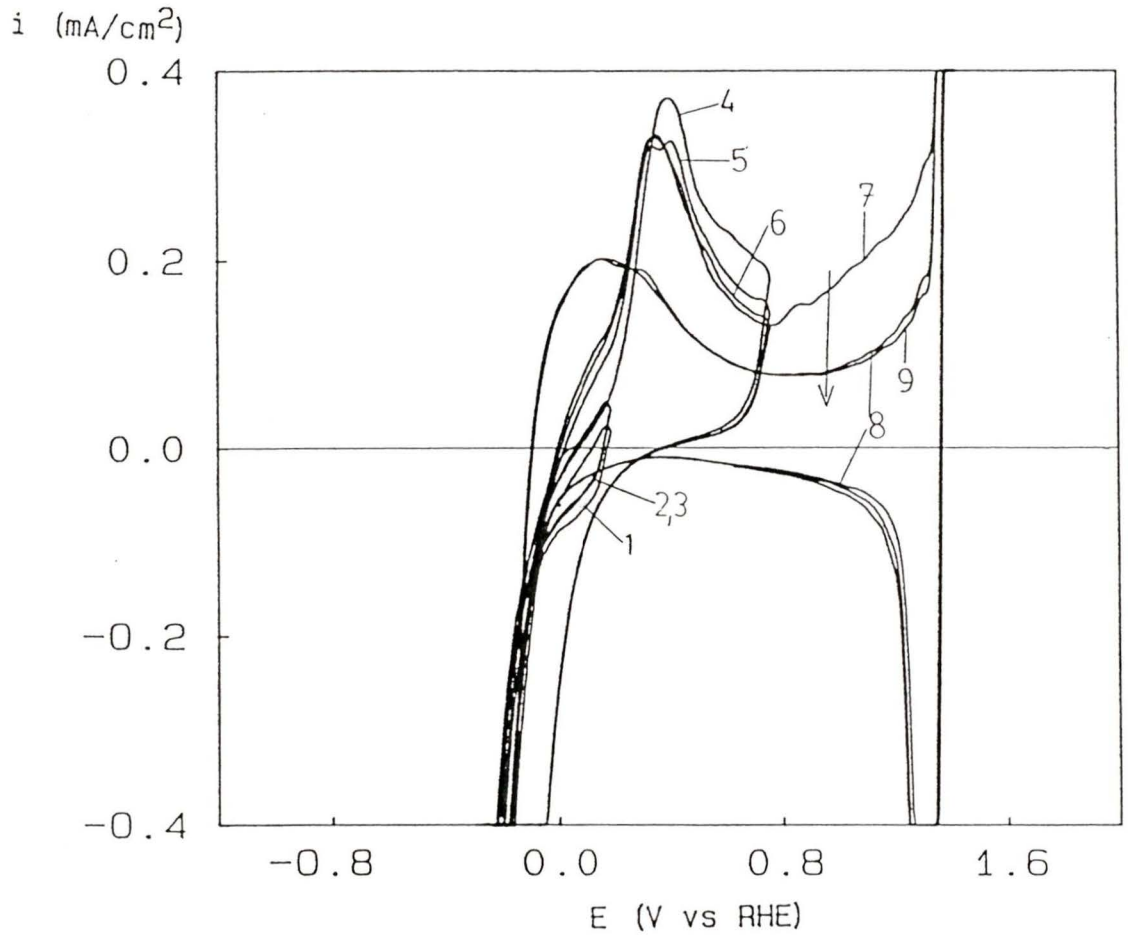

Figure 19: Cycles 1-9 of the Nickel Disk Electrode in 1M NaOH (MacDougall Preparation)

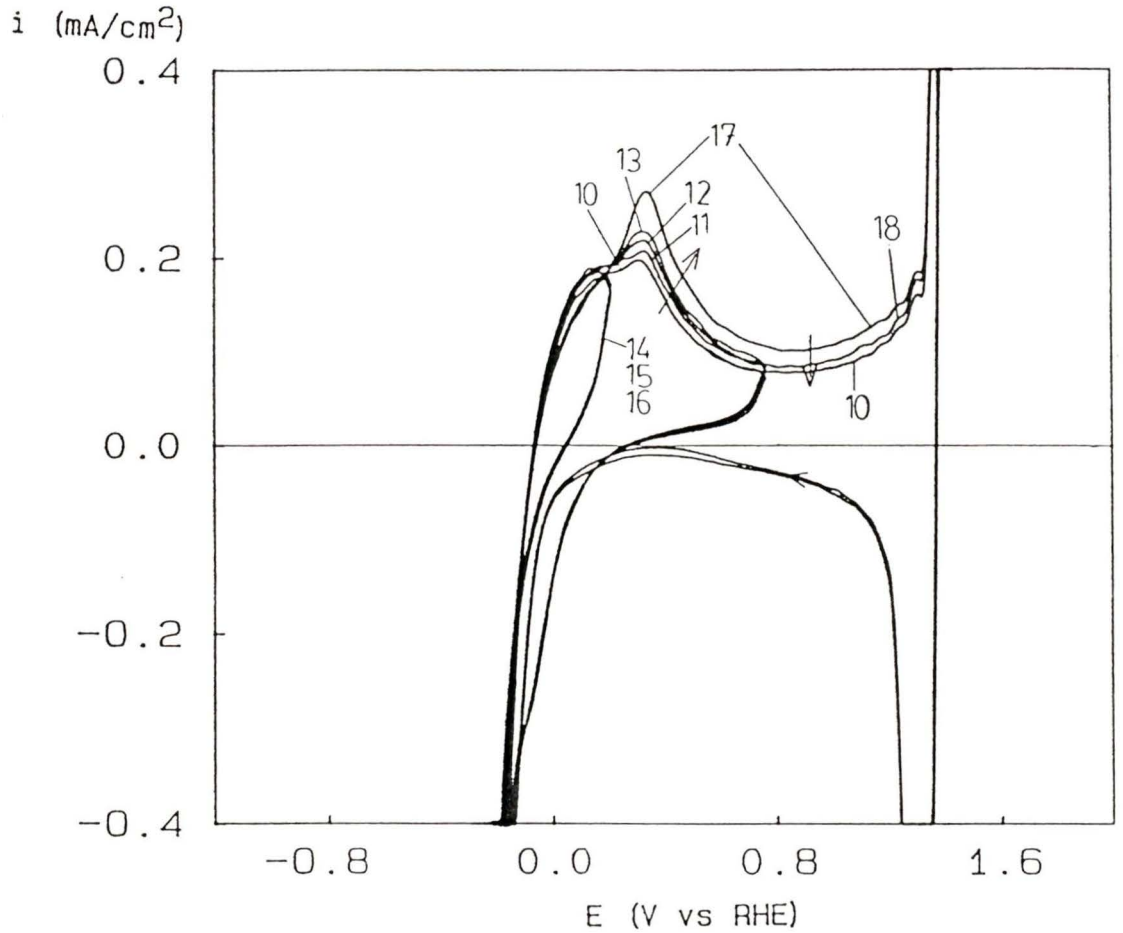

Figure 20: Cycles 10-18 of the Nickel Disk Electrode in 1M NaOH (MacDougall Preparation)

the surface seen for this electrode in the restricted cycling region.

The γ-oxyhydroxide reduction peak was also seen to contain a much higher charge density in the first few extended cycles compared to those seen in the elution experiments. Since the oxyhydroxide reduction requires insertion of protons and removal of water from between the layers of oxide [4], it should occur more readily in a less perfect film. This is because there is more room between the layers to allow diffusion of water out of the film, as well as the incorporation of protons back into it. This ultimately affects the rate of film reduction, and will be discussed in more detail further on.

There were no anodic excursions on the reverse sweeps. This seems to be a feature observed only in the elution experiments, but is not readily explained. The MacDougall electrode also shows the extra α' space peak just prior to the formation of the α-hydroxide. This peak is more clearly resolved in these cycling experiments than in the experiments involving the electrode prepared by the elution technique. The hypothesis that the peak is associated with nickel metal dissolution is perhaps supported by this

observation. The rougher electrode fabricated by the MacDougall procedure will probably have higher rates of dissolution of metal from the surface than from the smoother electrode made by the elution technique. It is clear that there are definite differences in the cycling behavior of the electrodes depending on the surface preparation used.

3.7 - Experimental Results with the Ni(111) Single Crystal Electrode in Aqueous Solution.

Experiments with the Ni(111) single crystal electrode were also performed, to see the effect of surface structure on cycling behavior. After the elution procedure, the first few cycles had behavior similar to that of the polycrystalline electrode studies in the 1.0M NaOH electrolyte. The main difference was in the *magnitudes* of the current densities. The (111) electrode showed at least a factor of 2 increase in the current density maximum for the α-hydroxide formation peak (see figures 21 and 22). Relative comparisons of the amount of oxide formed on the surfaces of all electrodes studied in aqueous studies can be seen in Table 3. When a comparison of the behavior of the electrode versus that seen in the cycling experiments of Beden and Lamy [20] for their (111) electrode (figure 22), our

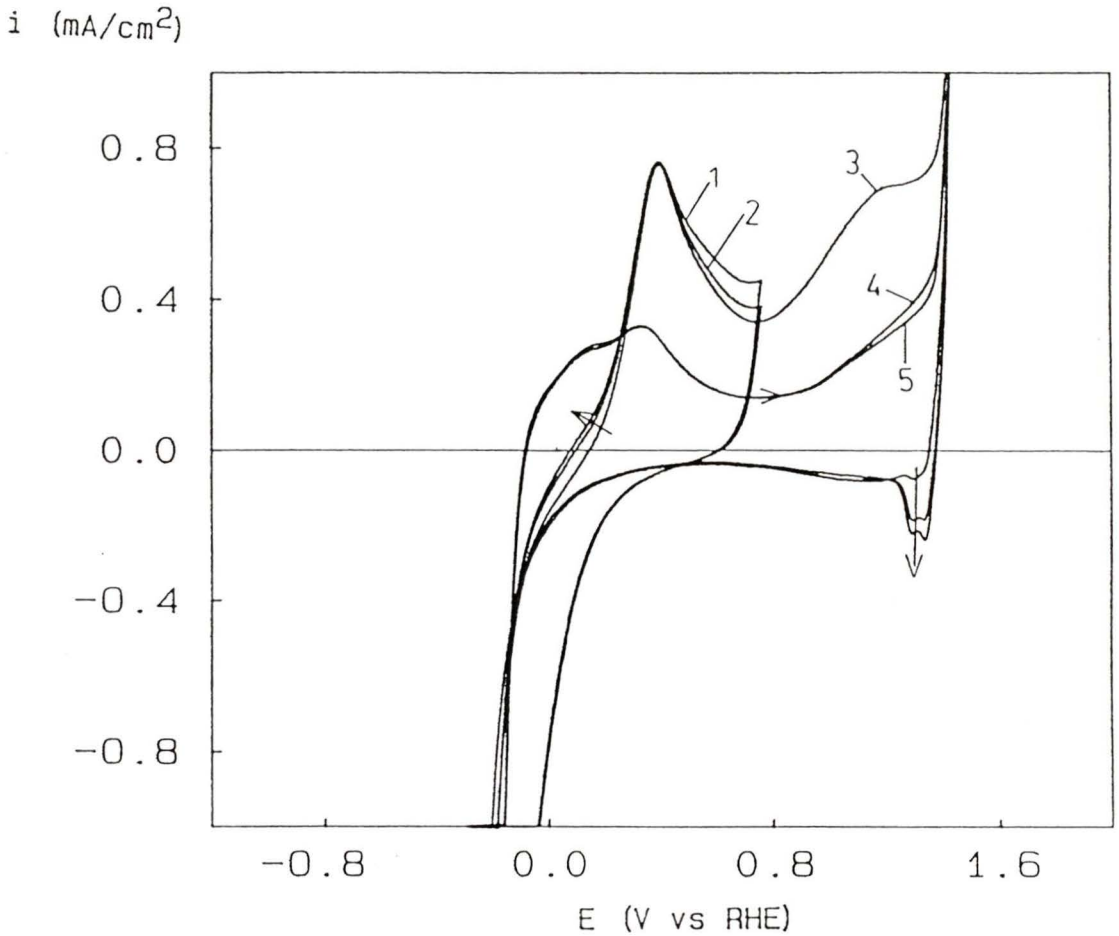

Figure 21: Cycles 1-5 of the Nickel(111) Electrode in 1M NaOH (Elution Procedure)

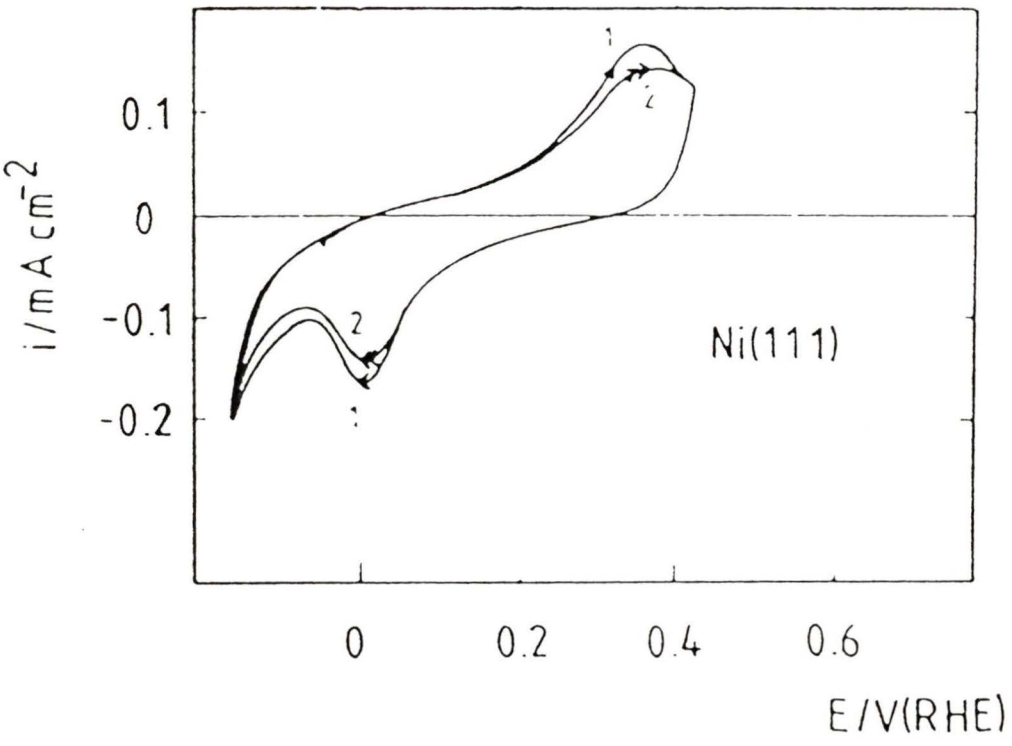

Figure 22: Beden and Lamy's Cyclic Voltammetry Results for their Nickel(111) Electrode (from ref[20])

electrode shows a greater current density by a factor of about 2.5 to 3.0 for the α-hydroxide peak. This indicates a greater surface reactivity for the (111) electrode than has been observed previously, presumably because our surface preparation leads to a surface nearer the oxide-free, ideal Ni(111) surface. A better surface may lead to a better epitaxial fit of the α-hydroxide on the surface, facilitating oxidation of the surface compared to other surfaces. The α-hydroxide peak shows fairly reversible cycling in the restricted potential region.

3.7.1 - Other Features Seen on Cycling the Ni(111) Electrode.

The shoulder peak near the α-peak appears after the first extended cycle to +1.5V, similar to the polycrystalline disk experiments. Virtually all the surface reactivity is regained on reversing the cycling trend to lower upper limit values gradually for a few cycles and then extending the range back to +1.5V. The area of the α-hydroxide peak is almost the same as that for the very first cycle to +0.8V, and this suggests the film is almost 100% reversibly reduced back to the metal (see figures 21 and 23).

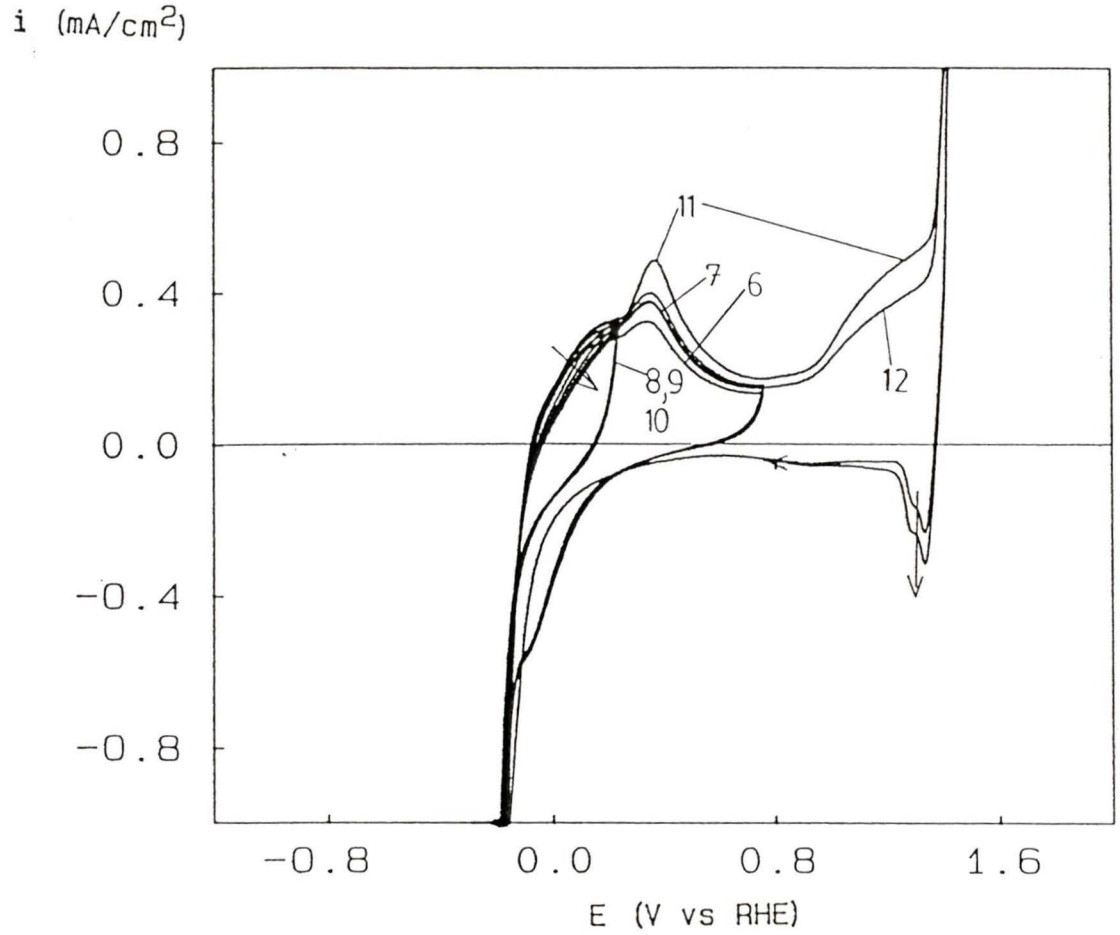

Figure 23: Cycles 6-12 of the Nickel(111) Electrode in 1M NaOH (Elution Procedure)

The observed resolution between the β and γ-oxyhydroxide reduction peaks was greater for the Ni(111) electrode. These were seen only as a peak and a broad plateau in the polycrystalline studies. There may be different activation energies for reduction of the Ni(111) surface films than for the activation energies required for the same film on the mixture of surface planes present in the polycrystalline electrodes. The γ-OOH reduction peak grows with cycling in the cycles going to +1.5V, indicating a gradual conversion of α and β-phases to the γ-oxyhydroxide phase is occurring.

There is a definite pattern in the ease of reduction of the γ-OOH phase. This may be quantified as the ratio of γ-OOH reduction current to α-OH peak oxidation current. The α-hydroxide charge is used as a reference to remove any complication due to changes in surface roughness, since both peaks change proportionately with changes in the roughness factor. The trend in the different surface preparations supports the hypothesis that surface films formed on smoother electrodes may be more highly ordered and more difficult to reduce. The roughest electrode, the one prepared by the MacDougall procedure, has the largest γ-OOH : α-OH ratio of the three electrodes studied in 1.0M NaOH. The disk electrode prepared by the elution technique had the

next largest ratio, and was also the next smoothest macroscopically. The smoothest electrode, the Ni(111) electrode, had the smallest ratio. This may be readily seen by comparing figures 16, 19 and 21.

It is known in the literature [4,16] that the reduction of the γ-oxyhydroxide involves electron transfer as well as proton insertion (for charge balance in the film) and removal of intercalated water from between the hydroxide sheets. The extremely rapid rise in current seen in the γ-OOH formation peak and the sharp drop in current at the most anodic region of the voltammograms during sweep reversal suggests that the redox processes are highly reversible and occur at very high rates. Perhaps the more well-ordered the surface hydroxide film is, the more difficult it becomes to reduce it, because it is more difficult for protons to diffuse back into the layers, and the removal of intercalated water becomes typically slower. The greater γ-OOH reduction charge is not due to a larger amount of film on the surface, since the oxidation charges are similar. A rough surface film will thus exhibit larger cathodic currents for the reduction of the γ-oxyhydroxide film back to the α-hydroxide, because the rates of proton insertion and water removal are typically higher.

3.8 - Nickel Disk Electrode Experiments in Acetonitrile.

When the solvent for the system was changed from water to acetonitrile, some interesting differences in the cycling behavior of the electrode were observed. There were traces of water in the solvent, and these could be used as a source of water for the formation of hydroxide films on the surface. The acetonitrile experiments differ from the aqueous experiments not only in water concentration, but also in pH - they were carried out at a nominal pH of 7 rather than pH 14. This was necessary, because it was experimentally determined that dry NaOH was virtually insoluble in AN. It was physically impossible to achieve a $[OH^-]$ of 1.0M.

The α-hydroxide is not well resolved in any of the cycling experiments. As can be seen in figure 24 , the hydrogen evolution reaction is also not very facile in the acetonitrile solvent. This is observed in the lower current densities per cycle compared to those seen in the aqueous experiments (compare table 3 with table 4). This indicates that the concentration of water at the surface is involved in the rate expression for the process. The cathodic

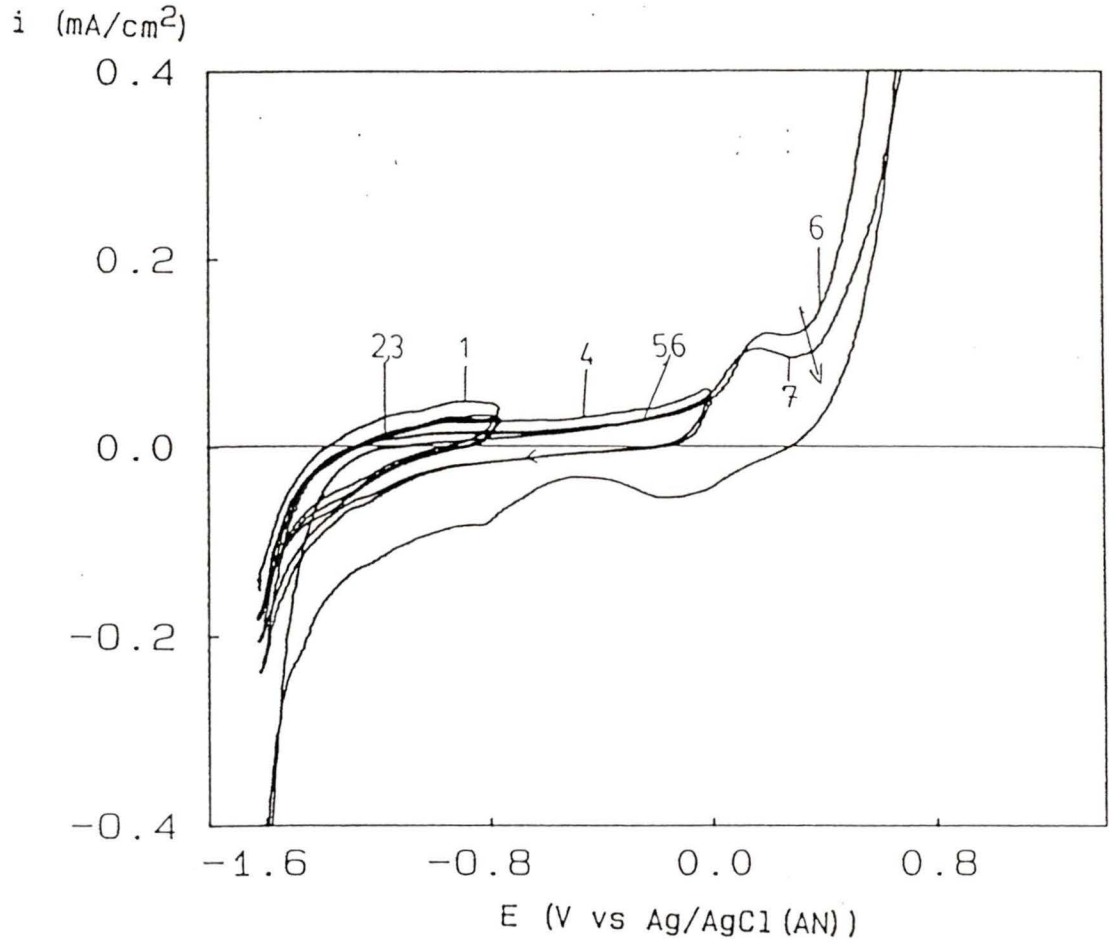

Figure 24: Cycles 1-7 of the Nickel Disk Electrode in Acetonitrile (Elution Procedure)

Table 4: Charge Density Data for the Acetonitrile Systems

Ni Disk ["Dry" AN]	Q_a (mC/cm^2)	Q_c (mC/cm^2)	ΔQ (mC/cm^2)	Net oxide coverage, monolayers
cycle: 1	0.34	0.27	0.07	0.13
2	0.19	0.31	-0.12	-0.22
4	0.60	0.62	-0.02	-0.04
6	4.86	1.77	3.09	5.56
14	1.83	1.46	0.37	0.67
15*	0.26	0.55	-0.29	0.52
20*	13.01	2.24	10.77	19.37
21*	7.55	2.09	5.46	9.82
Ni Disk AN [1% water]	**Q_a (mC/cm^2)**	**Q_c (mC/cm^2)**	**ΔQ (mC/cm^2)**	**Net oxide coverage, monolayers**
cycle: 4	1.33	1.01	0.32	0.58
5	1.17	1.14	0.03	0.05
6	6.05	2.00	4.05	7.28
11	2.33	1.24	1.09	1.96
12*	2.52	1.03	1.49	2.68
19*	12.57	3.90	8.67	15.59
20*	8.46	3.40	5.06	9.10
Ni(111) ["dry" AN]	**Q_a (mC/cm^2)**	**Q_c (mC/cm^2)**	**ΔQ (mC/cm^2)**	**Net oxide coverage, monolayers**
cycle: 4	0.41	0.53	-0.12	-0.20
5	0.67	0.58	0.09	0.15
6	0.67	0.59	0.08	0.13
7	2.13	0.59	1.54	2.58
9	9.27	1.60	7.67	12.87
11	2.40	1.93	0.47	0.79
12**	3.60	2.21	1.39	2.33
13	0.26	----	----	----
15	0.22	0.85	-0.63	-1.05
19	9.98	2.72	7.26	12.18

*cycles went offscale at the γ-OOH region; this is the minimum amount of oxidation charge density for the cycle.

**the scope trace ended during cycle 13; the reduction current density data was unavailable for this cycle.

reaction at the most negative potentials of the voltammogram is assigned to the H.E.R. because the potential scales of both solvent systems nearly line up in this region. Furthermore, the H.E.R. is considered to occur in this potential region because the solvent breakdown does not occur until more negative potentials are reached [28]. The Ag/AgCl reference electrode used has a potential of 297±7mV (vs SHE; this is the average between the calculated and experimentally derived values). The common potential scale employed in the comparison between the different solvent systems was the SHE scale, and the zero potential values for each system were lined up to make a qualitative comparison of the behavior of both solvent systems.

The hydrogen evolution reaction seems to be enhanced with further cycling, and is more facile after the electrode has been more completely oxidized. It is possible that the hydroxide itself may promote or enhance hydrogen evolution at the electrode surface. The enhancement of the H.E.R. rate on pre-oxidized surfaces was first proposed in a paper by A. Lasia [29]. An alternative proposal is that the local water concentration is increased by oxide reduction, thus increasing the rate of decomposition of water to hydrogen. Assuming the former explanation, the maximum H.E.R. current

observed must be less than the diffusion-limited current bringing water to the surface. This allows a lower limit estimate on the concentration of water in the solution, since mass transfer is a known function of the rotation rate of the rotating disk electrode. Taking the maximum H.E.R. current in figure 24 (offscale on the figure: 970$\mu A/cm^2$), and assuming a diffusion coefficient D = 10^{-5} cm^2/s, a kinematic viscosity of 0.439 x 10^{-2} cm^2/s, and a disk rotation rate of 21 rad/s (angular velocity used instead of the 33Hz rotational frequency), we calculate using the Levich equation [31] a minimum water concentration of 7.71 mM, or 0.04 % mole fraction.

The oxidation of the surface to the α-hydroxide occurs at more negative potentials (versus the H.E.R.) in acetonitrile than in aqueous solution. The potentials at which the oxidation of the surface is observed coincides with potentials at which hydrogen evolution is still occurring in the corresponding aqueous experiment. This supports the hypothesis that α-formation can indeed occur concurrent with the hydrogen evolution reaction. Previous to this study, little (if any) direct evidence existed to support the above proposition on the behavior of nickel at these potentials.

A well-defined peak for oxidation of the hydroxide films to the β-oxyhydroxide is observed in acetonitrile (see figures 24 to 28). This feature is usually present but less defined in aqueous experiments. For sequential processes (such as the oxidation of β-OH to β-OOH and finally to the γ-OOH), it is expected that if the kinetics are slower, the peaks will be better resolved. Also, the rise toward the γ-OOH peak is not nearly as steep as the rise in the corresponding aqueous work, and the reduction of the film is seen as a shallow peak *without* the presence of the sharp reduction peak typically seen in 1.0M NaOH. All observations suggest slower redox processes in acetonitrile. As in the case of the hydrogen evolution reaction, slower kinetics imply involvement of the concentration of water in the rate law. Oxidation of the hydroxides to the oxyhydroxides and their corresponding reduction involve migration of both protons and water within the film [4]. Water migration is likely slower than proton migration, and we might therefore expect the water concentration at the electrode surface to influence the kinetics.

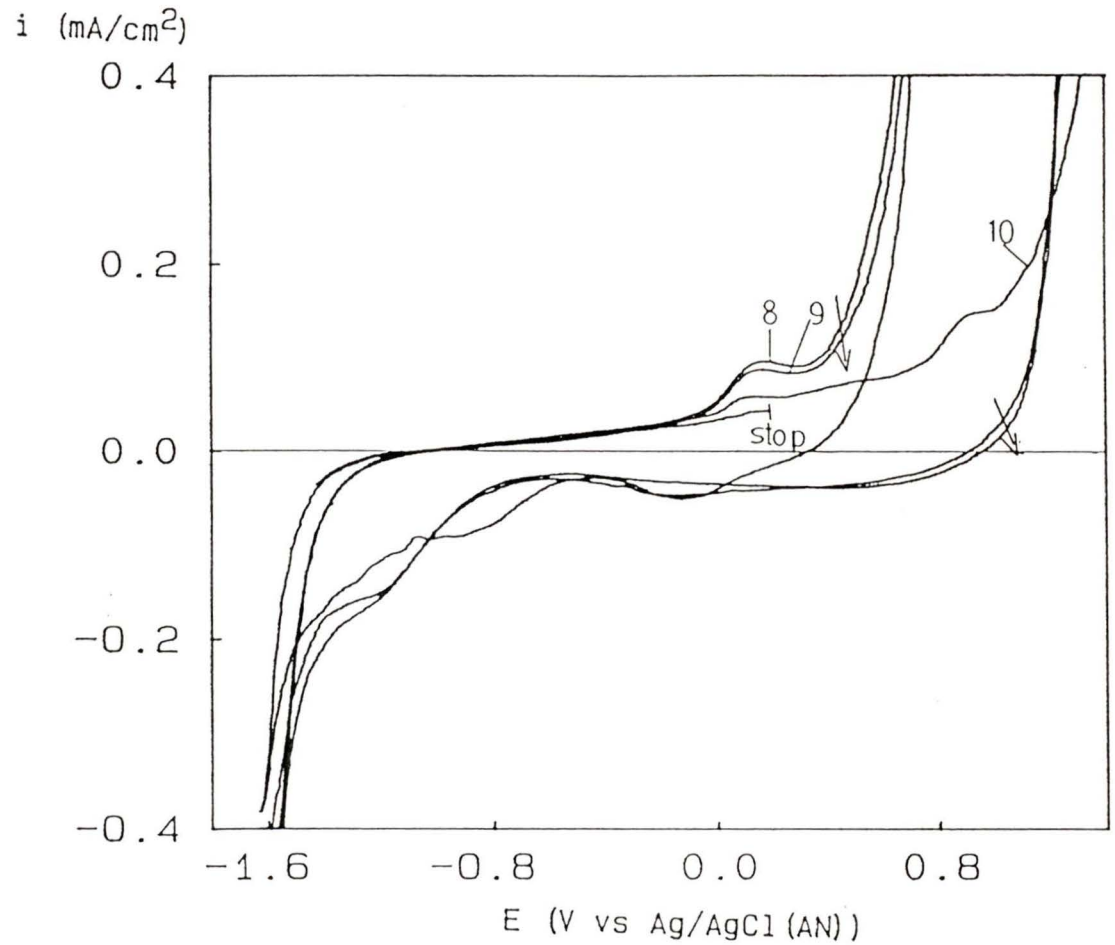

Figure 25: Cycles 8-10 of the Nickel Disk Electrode in Acetonitrile (Elution Procedure)

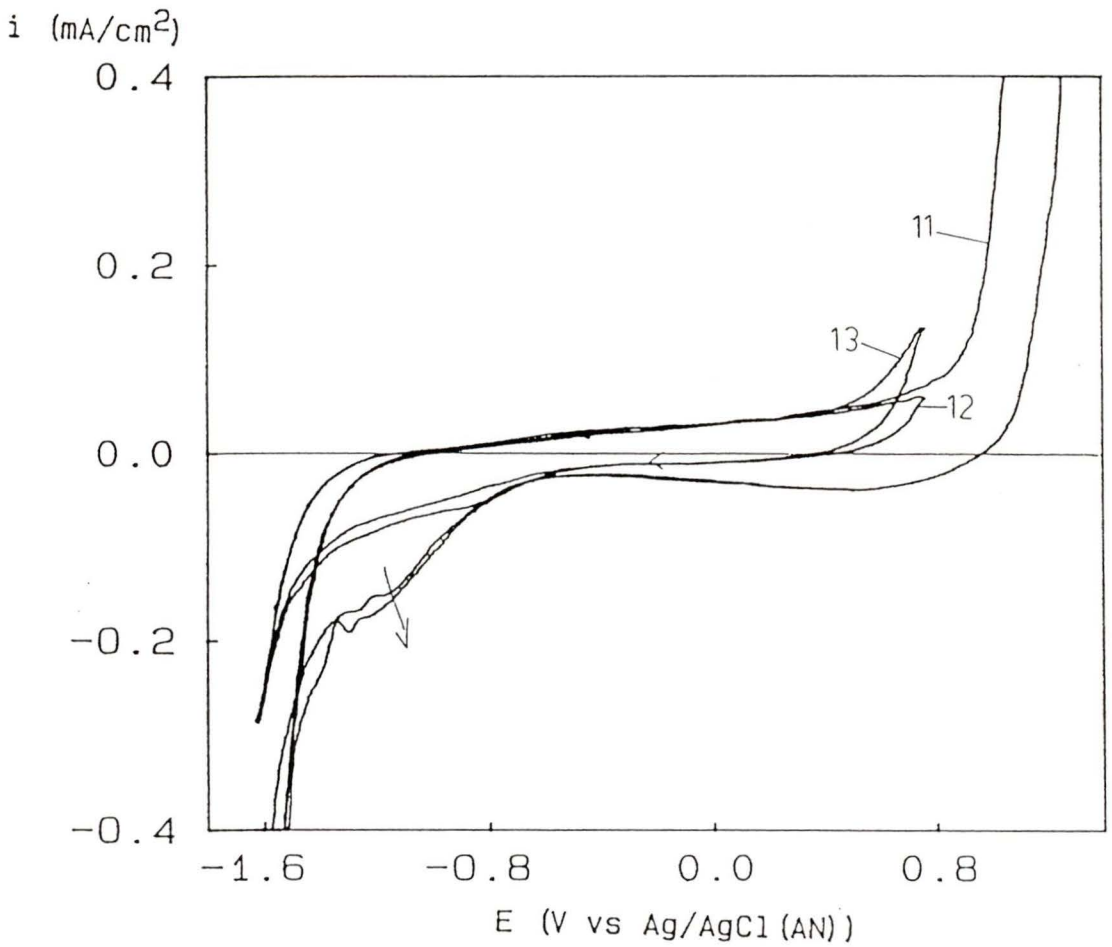

Figure 26: Cycles 11-13 of the Nickel Disk Electrode in Acetonitrile (Elution Procedure)

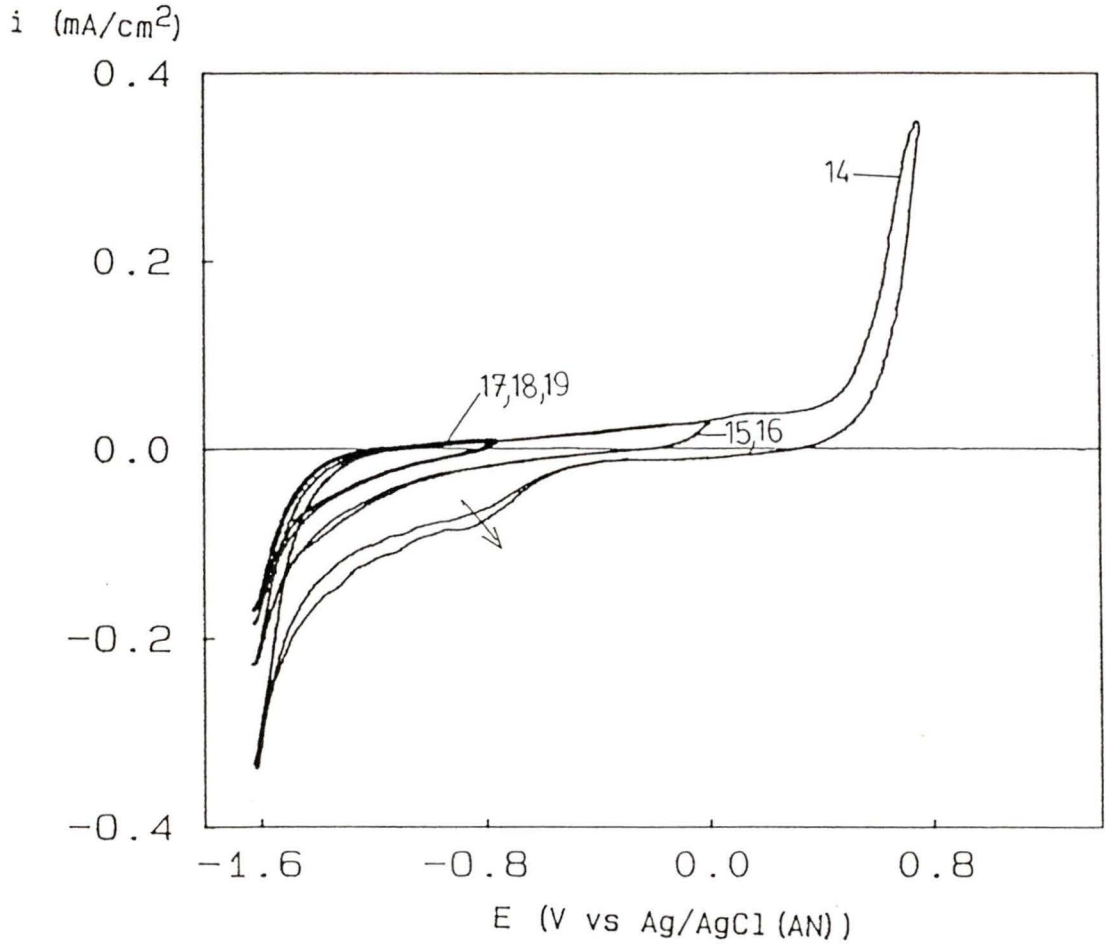

Figure 27: Cycles 14-19 of the Nickel Disk Electrode in Acetonitrile (Elution Procedure)

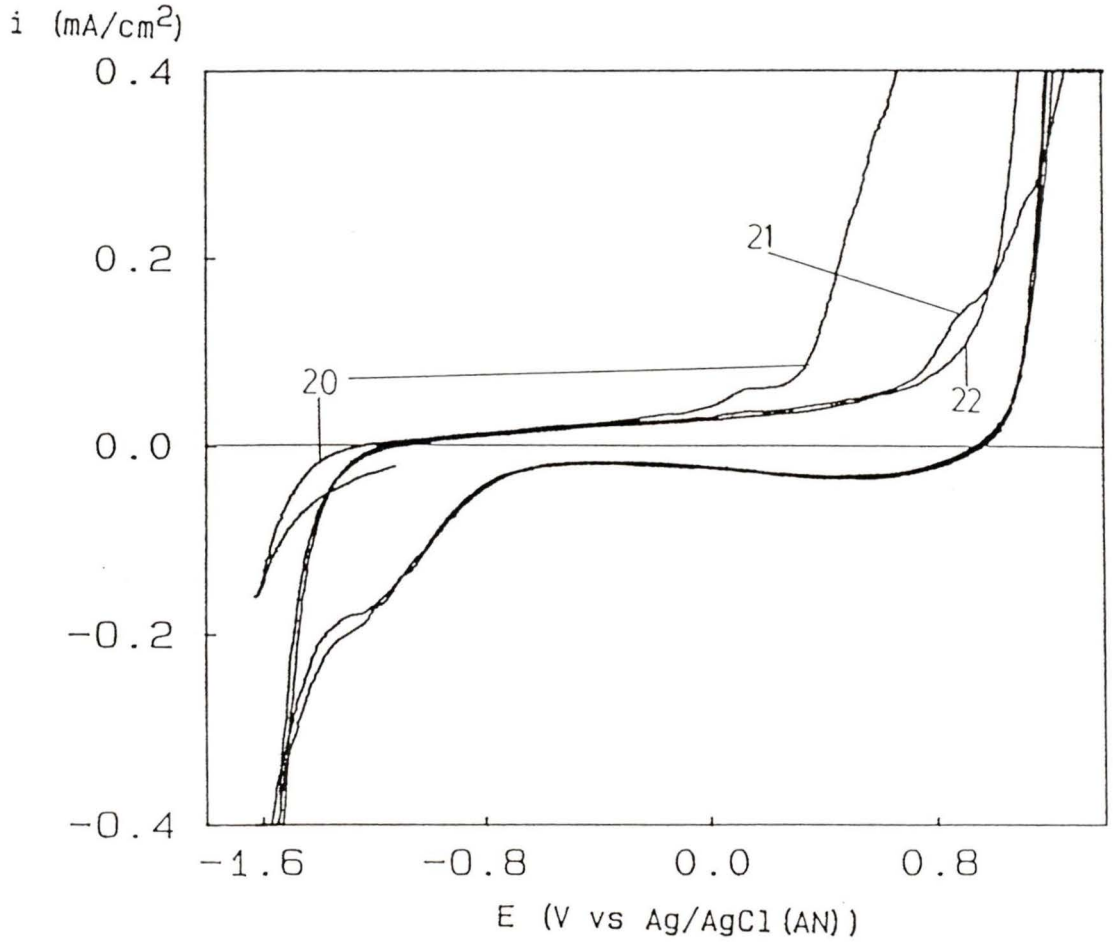

Figure 28: Cycles 20-22 of the Nickel Disk Electrode in Acetonitrile (Elution Procedure)

3.8.1 - Results After Water Addition to Disk Electrode in Acetonitrile.

Water (about 0.5mL) was added to the AN solution immediately following the elution procedure in an experiment used to study the effect of increasing the local water concentration on the disk electrode.

The peaks are observed to be enhanced during cycling over the same potential range as was used for the Ni/AN system previously. They also increase proportionately, with no evidence for enhancement of selected peaks. The H.E.R. current on the reverse sweep goes off scale at about -1.2V (see figure 29). This supports the hypothesis that the H.E.R. was limited in the previous experiment by the local water concentration near the surface. Higher water concentrations in the cell allow the reaction to progress at much higher rates.

An anodic shift in the potential of the H.E.R. on the return sweep is also observed when water is added to the system (see figures 29 to 32). This shift towards the reversible potential can be attributed to the hydrogen evolution reaction becoming more facile. However, the

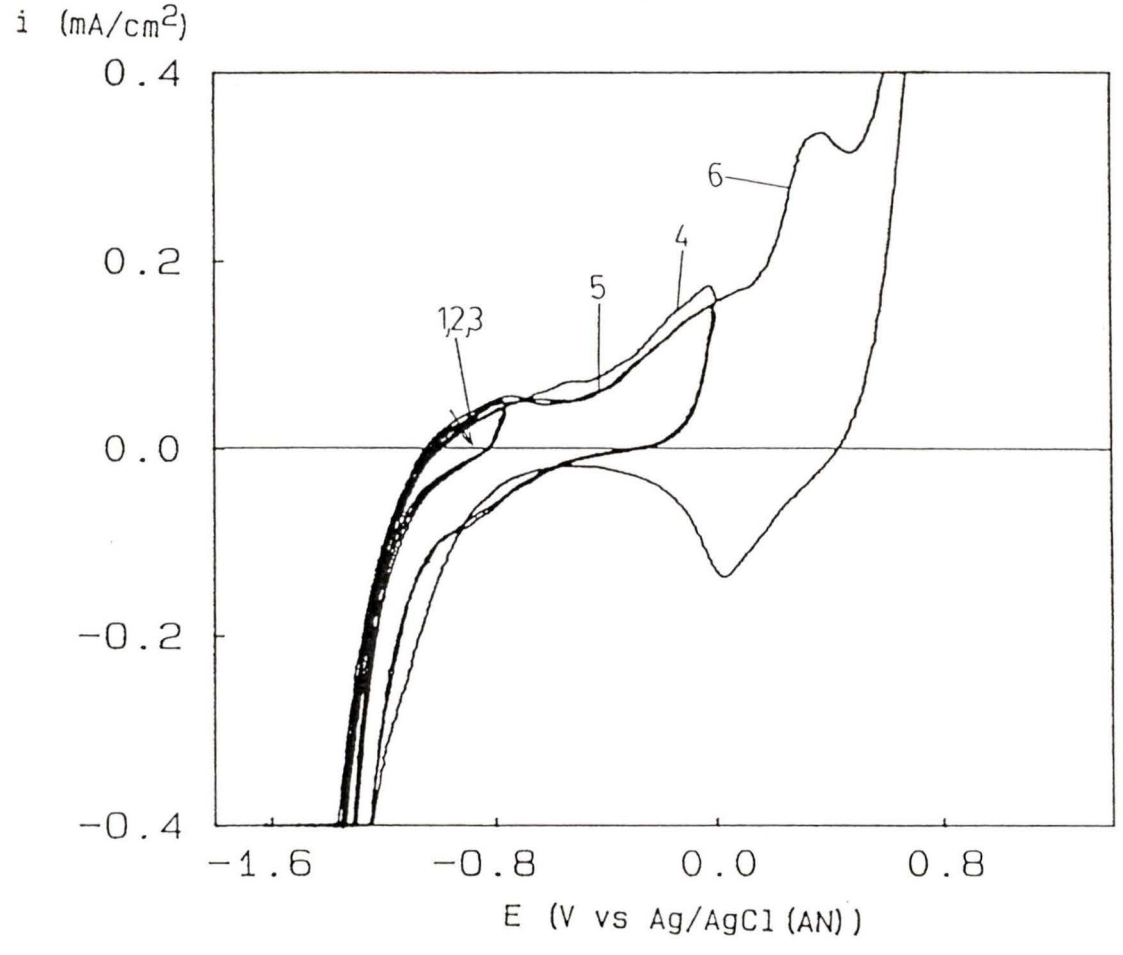

Figure 29: Cycles 1-6 of the Nickel Disk Electrode in Aqueous Acetonitrile (Elution Procedure)

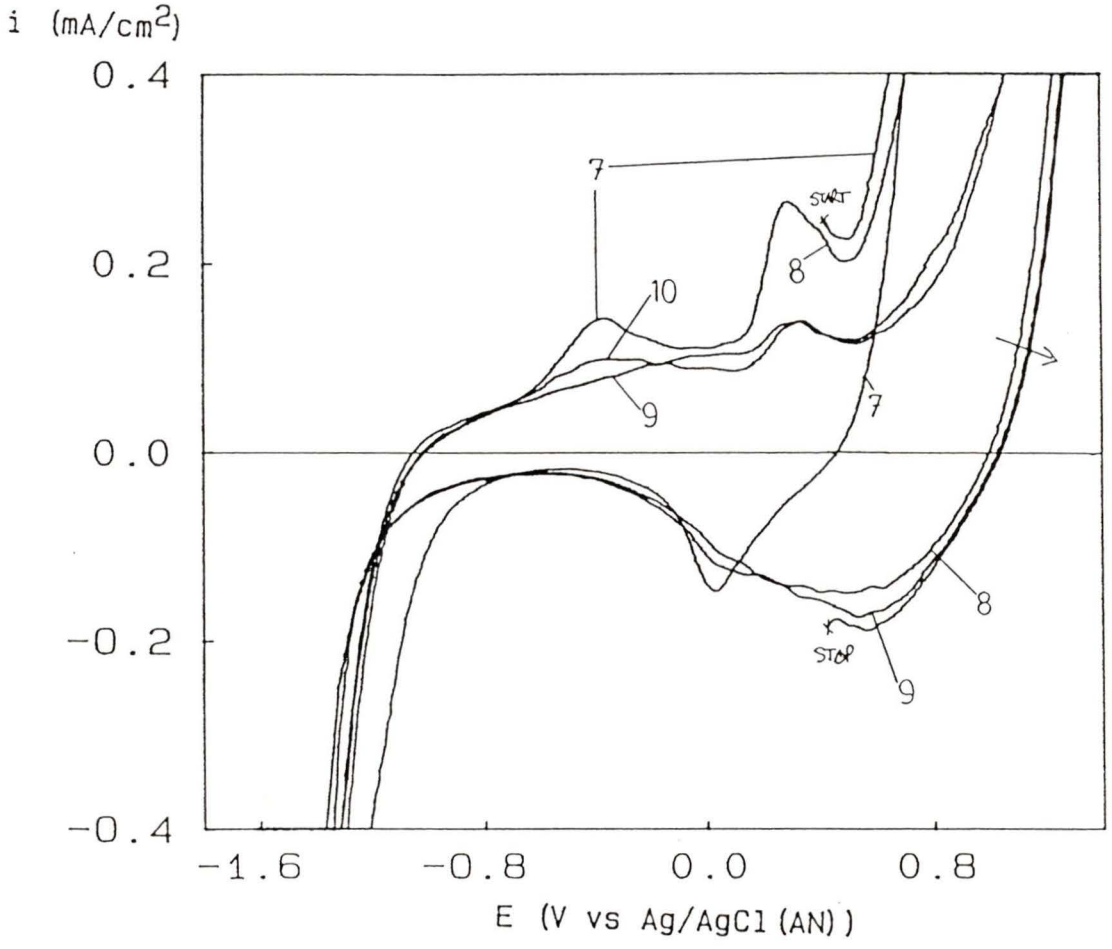

Figure 30: Cycles 7-10 of the Nickel Disk Electrode in Aqueous Acetonitrile (Elution Procedure)

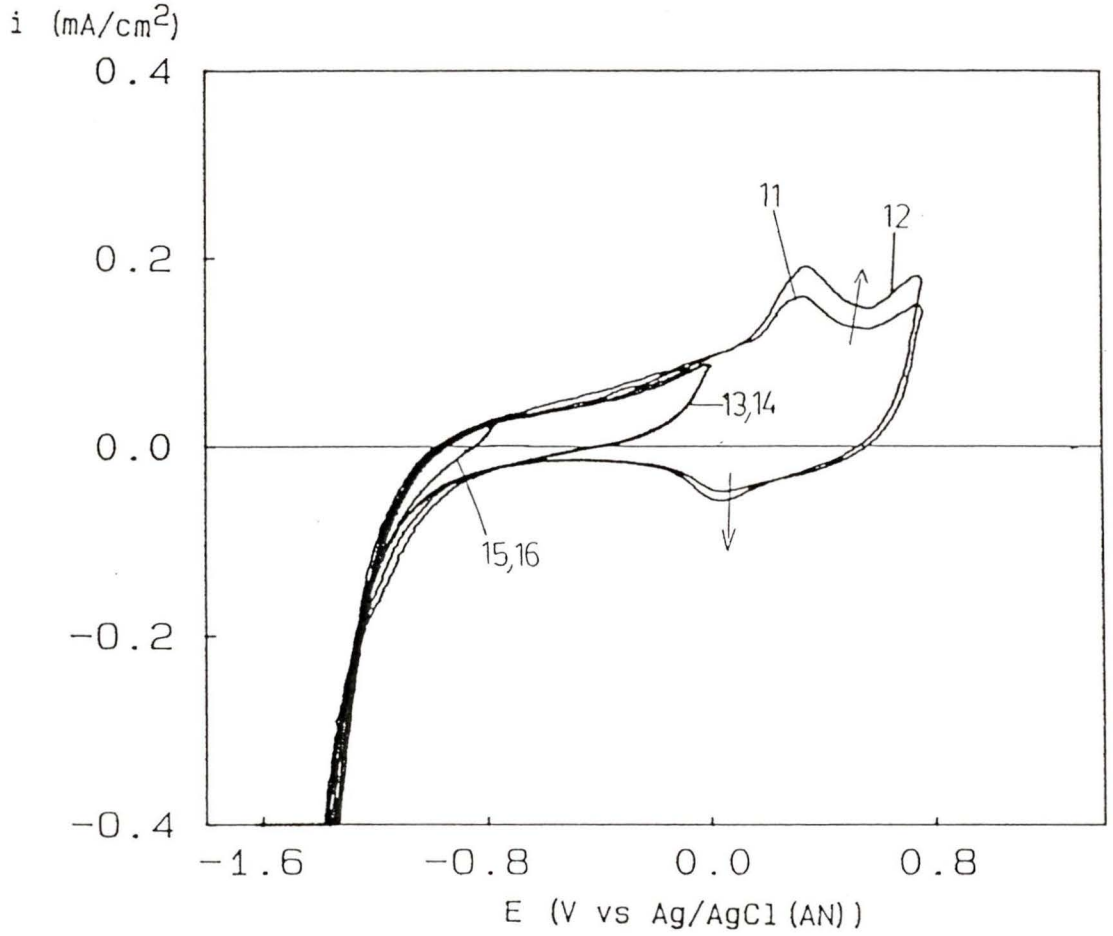

Figure 31: Cycles 11-16 of the Nickel Disk Eletrode in Aqueous Acetonitrile (Elution Procedure)

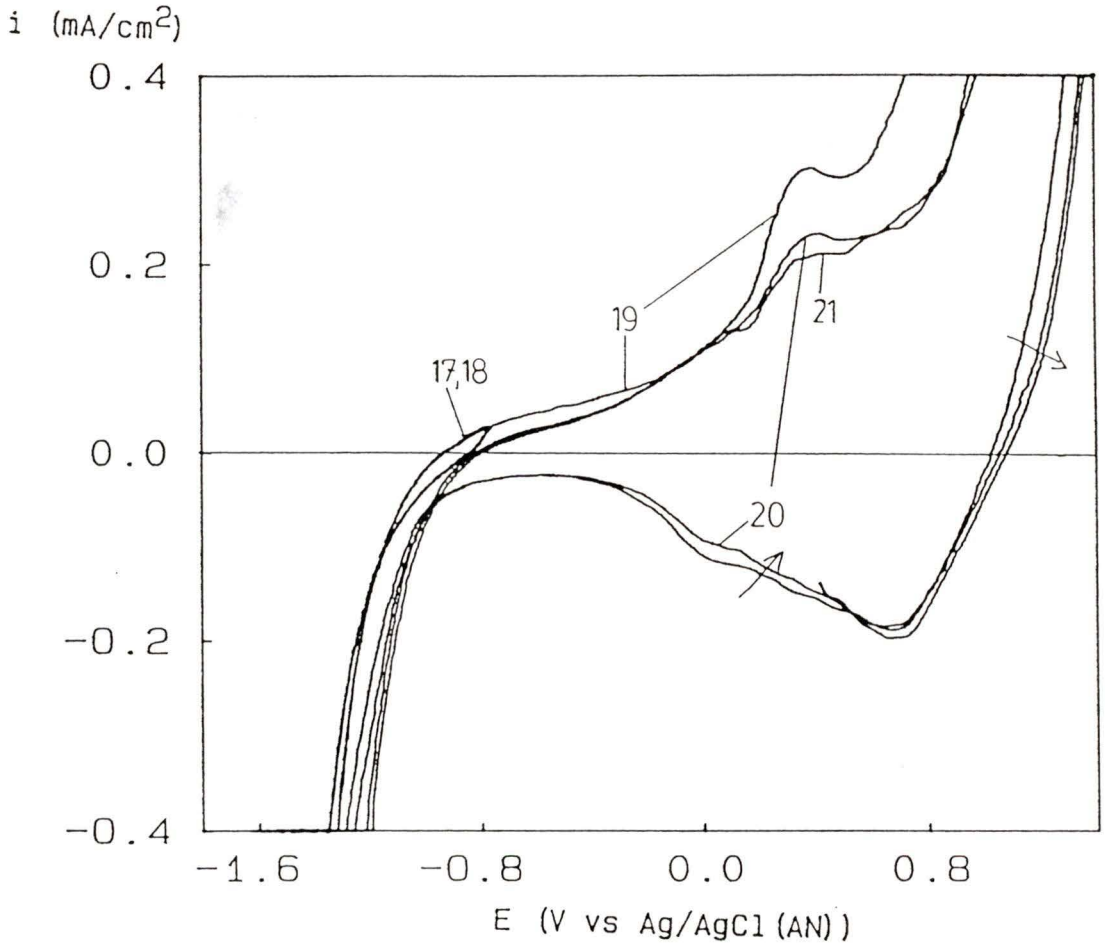

Figure 32: Cycles 17-22 of the Nickel Disk Electrode in Aqueous Acetonitrile (Elution Procedure)

concentration of water is not sufficiently high for similar behavior to aqueous solutions. For example, the potential limits of the H.E.R. and the γ-OOH formation reaction are further apart in the AN/H_2O system than they are in the aqueous system (see figures 16, 19, and 29), but some of this difference is due to the slower kinetics of the γ-OOH formation. They are, however, less far apart than the potential limits for the two reactions observed in the AN system alone. There exists a continuity in the behaviors of the three systems, where both the magnitude of oxidation charges and speed of the reactions at the surface seem to be dependent on the amount of water present at or near the electrode surface. It is clear that water plays a key role in the redox behavior of nickel and its oxides. Further kinetic studies using other transient electrochemical techniques could be used to determine further mechanistic details of the system.

3.8.2 - Results for the Ni(111) Single Crystal Electrode in Acetonitrile

The behavior of the Ni(111) single crystal in acetonitrile is virtually the same as that for the disk electrode in AN (see figures 16 and 33). This suggests that

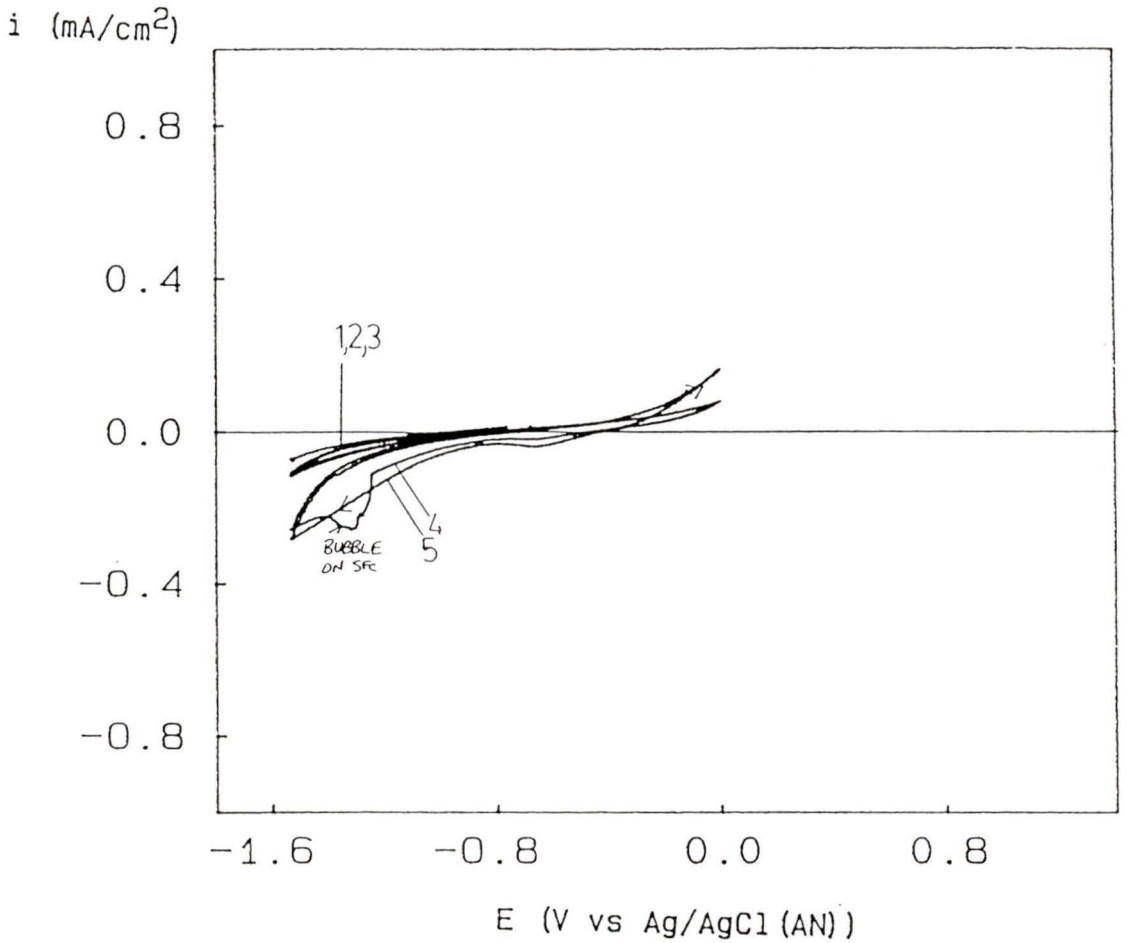

Figure 33: Cycles 1-5 of the Nickel(111) Electrode in Acetonitrile (Elution Procedure)

the structural effects on cycling seen in the the aqueous systems studied are not as important in AN. This may be due to the fact that diffusion of water in approaching the surface of the electrode limits the rate of the reactions occurring on the surface (e.g. the H.E.R.), thereby masking any structural effects that would otherwise be present. In aqueous solution, the diffusion limiting effect is not present, and structural effects on the cycling behavior of the electrode were indeed observed for the well-ordered Ni(111) electrode in 1.0M NaOH (compare figures 16 and 21 with figures 24 and 33.).

For completeness, the cycling behavior of the Ni(111) electrode is included in figures 34 to 37. The cycling sequence is the same as that used in all previous experiments. Very little change in the surface behavior was evident when the system was subjected to cycling in the full potential range both before and after restricting cycling to between -1.6 and -0.8V (see figures 34 and 37). This may indicate that the surface film formed was irreducable, since there was no observed increase in surface reactivity upon cycling again in the full potential range (-1.6 to +1.5V). This supports the hypothesis that the film formed on the smoother surface is more ordered and is closer to the

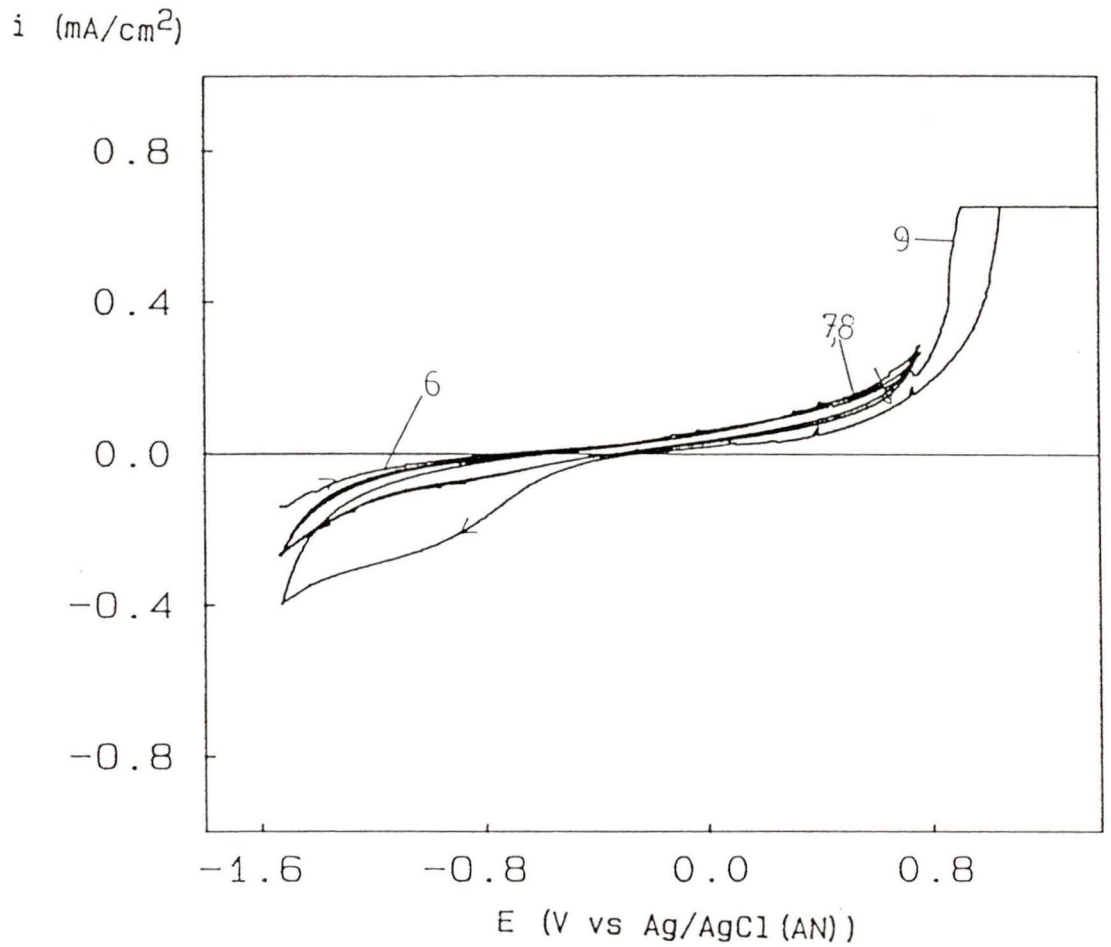

Figure 34: Cycles 6-9 of the Nickel(111) Electrode in Acetonitrile (Elution Procedure)

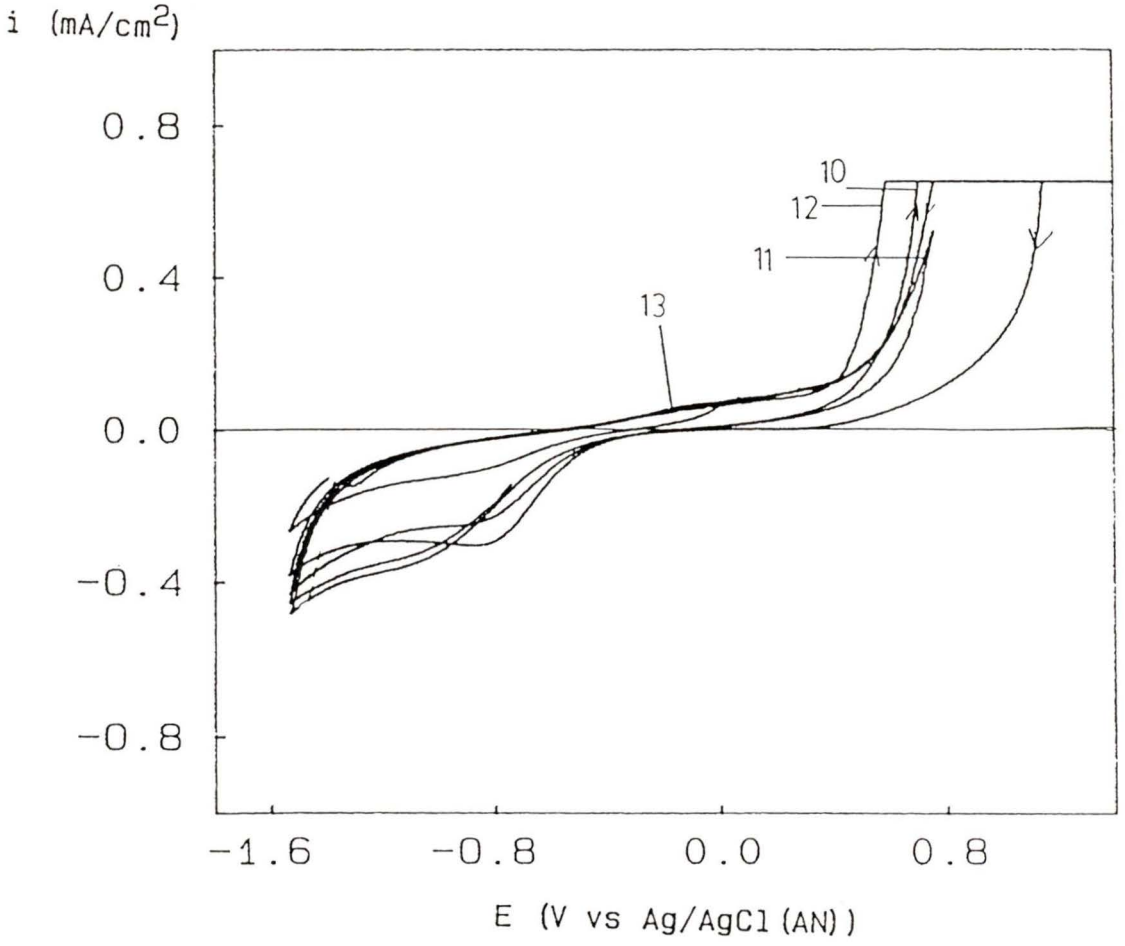

Figure 35: Cycles 10-13 of the Nickel(111) Electrode in Acetonitrile (Elution Procedure)

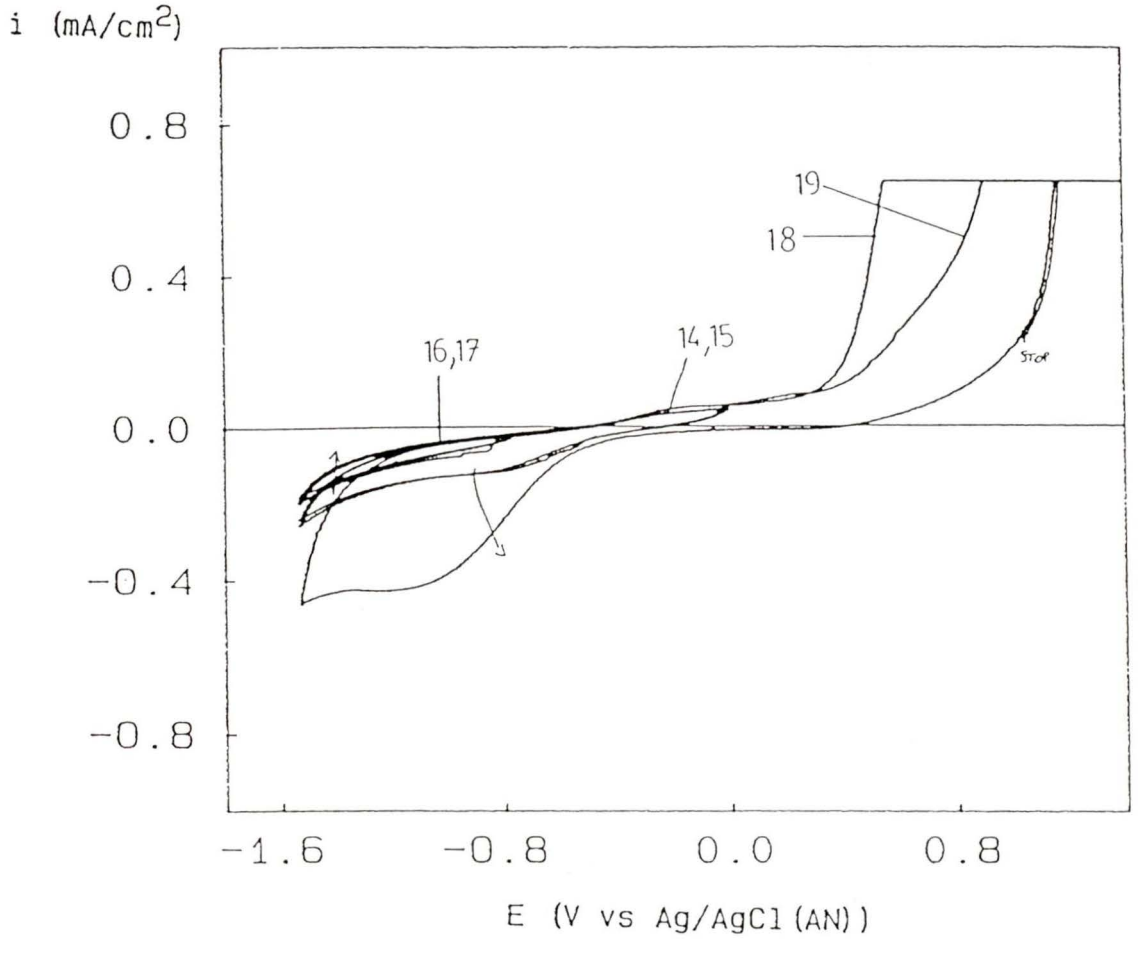

Figure 36: Cycles 14-19 of the Nickel(111) Electrode in Acetonitrile (Elution Procedure)

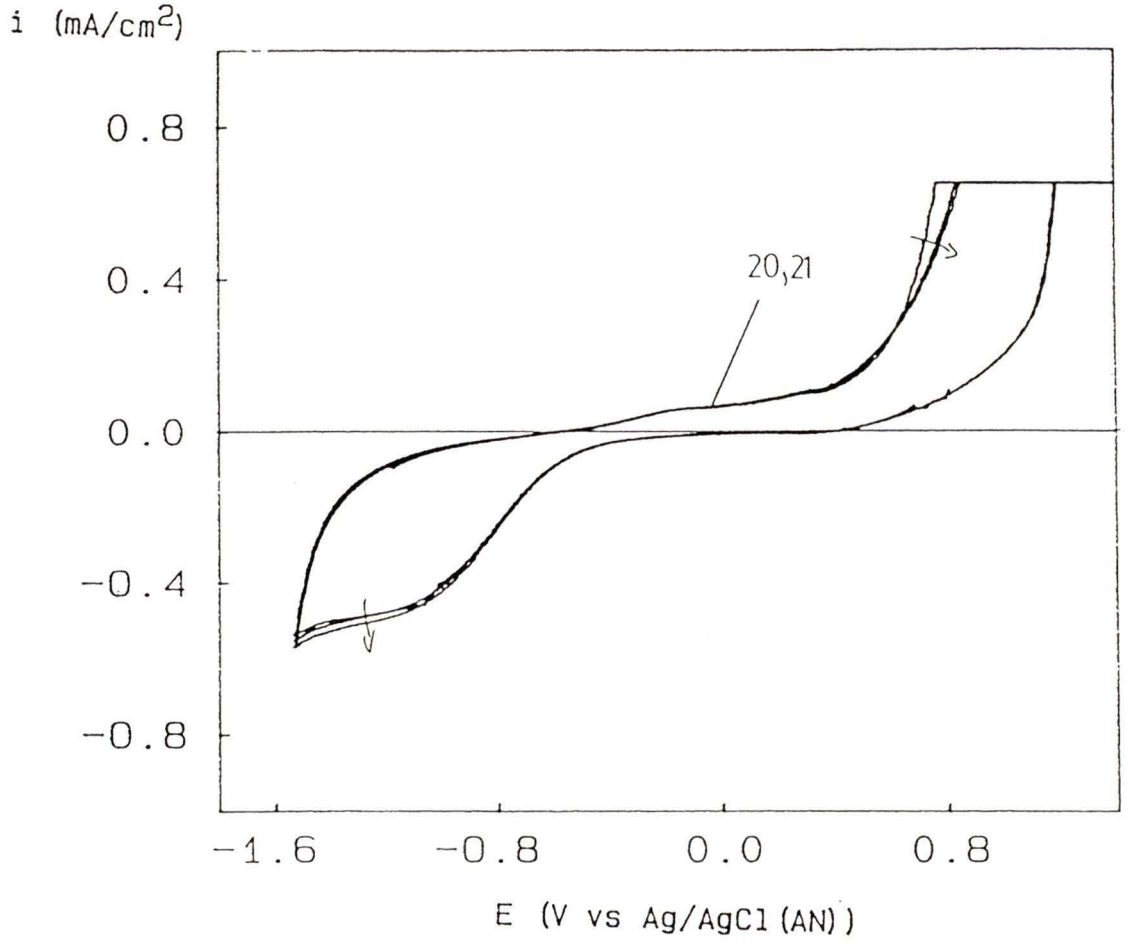

Figure 37: Cycles 20 and 21 of the Nickel(111) Electrode in Acetonitrile (Elution Procedure)

β-hydroxide in structure, therefore making it more difficult to reduce electrochemically. The peak on the negative-going sweeps in the cyclic voltammograms at -0.8V may be due to the reduction of any α-hydroxides formed on the surface. Further studies on the system may verify this.

Conclusions

The data taken on all the nickel electrode systems seem to suggest three main things about the behavior of nickel:

(1) The elution procedure appears to give a smooth, oxide-free surface. In the polycrystalline studies a more complete conversion of the α-OH to the irreducable β-phase was achieved as evidenced by the excess oxidation current densities observed. The smoother the electrode, the more ordered the hydroxide phase is, and, the closer it resembles the crystalline β-phase. If there were traces of the α-OH phase on the electrode surface *before* the cyclic voltammetry experiments, it would undoubtedly aid the formation of a less ordered surface hydroxide layer, since the newly-formed hydroxide sites on the surface would tend to adopt the crystallography of the layers adjacent to and below them. The fact that the Ni(111) electrode exhibited a higher degree of reactivity towards oxidation to the α-hydroxide may also suggest that the elution procdure employed in this study indeed may leave the surface more free from oxide than other surface preparations in the literature.

(2) Redox reactions at the surface of nickel have rates that depend very strongly on the concentration of water near the surface of the electrode [4]. Diffusion of water to the surface seems to be the rate-determining step in the hydrogen-evolution reaction, and diffusion of water away from the surface or through the film may be rate-limiting in the case of the γ-OOH reduction reaction. As the solvent system contains progressively larger concentrations of water, the diffusion effects become progressively less important, until the system approaches the behavior of Ni in aqueous solution. Effects of surface structure on cycling begin to appear only when these diffusion limitations are no longer important to the rate of the reactions.

(3) Effects of the surface structure on the cycling behavior of the electrode are important in the aqueous alkaline systems. The Ni(111) single crystal electrode exhibits increased reactivity towards the formation of the α-hydroxide phase. This may be due to the fact that the epitaxy of the crystalline β-phase may most closely match the alignment and orientation of atoms on the surface of the electrode. As a consequence, a larger number of crystalline layers may be deposited on this surface than on any other.

Suggestions for Future Work on this System.

Much more work can be done in future investigations of this system by studying the kinetics of α-hydroxide formation with cycling. A further study of what process is occurring in the α′ peak will shed further light on the electrochemical behavior of nickel in aqueous alkaline solutions, and the oxidation processes which are initiated in these solutions. A combined electrochemical/UHV experiment could be employed to study the surface at various stages of the elution to see what effects the elution has on preserving an oxide-free electrode surface. Better characterization of the surface areas of the electrodes used will undoubtedly be useful in coming to more precise conclusions as to the improvements the elution procedure offers to the study of oxide-free nickel electrodes.

Also, much work can be done in extending the present knowledge of the behavior of the higher oxide films, especially when such a clear separation between the reduction processes seems to be observed with the Ni(111) electrode. Further studies on the surface effects of cycling may allow for better characterization of processes difficult to separate from cycling experiments with polycrystalline

electrodes. These may then be more completely studied using potential-step and ac impedance experiments.

Finally, the experiments in acetonitrile may be continued by firstly trying to achieve drier solvent conditions. More precise measurement of the amounts of water present in the solvent will allow for more detailed study of the degree to which the diffusion of water is important in the surface redox reactions at the nickel electrode. A more detailed study could include cycling studies from dry acetonitrile to aqueous systems. The dry acetonitrile systems may then be modified by adding some surface-active agents known to impede the rates of corrosion, or some "modified" water molecules such as the primary alcohols. The effects of their introduction on the surface oxidation reactions could be studied.

REFERENCES

(1) Bode, H., Dehmelt, K., Witte, Electrochimica Acta, **11**, 1079 (1966).

(2) Weininger, J. L., Breiter, M. W., Journal of the Electrochemical Society, **110**, 484, (1963); **111**, 707 (1963).

(3) Bourgault, P. L., Conway, B. E., Canadian Journal of Chemistry, **38**, 1557 (1960)

(4) Oliva, P., Leonardi, J., Laurent, J.F., Delmas, C., Braconnier, J.J., Figlarz, M., Fievet, F. and deGuibert, A., Journal of Power Sources, **8**, 229-255 (1982)

(5) Structure Reports, vol 13, A.J. Wilson (ed.), International Union of Crystallography, Utrecht, 1950, p213.

(6) Structure Reports, vol 11, A.J. Wilson (ed.), International Union of Crystallography, Utrecht, 1947, p306.

(7) Pandya, K.I., Hoffmann, R.W., McBreen, J. and O'Grady, W.E., Journal of the Electrochemical Society, **137**, 383 (1990)

(8) Cabannes-Ott, C., Ann. Chim., **5**, 905 (1960)

(9) Schrebler-Guzman, R. S., Vilche, J. R., Arvia, A. J., Journal of Applied Electrochemistry, **9**, 183 (1979)

(10) Melendres, C. A., Paden, W., Tani, B., Walczak, W., Journal of the Electrochemical Society, **134**, 762.(1987)

(11) Zedner, J. Z. Elektrochem., **46**, 809 (1905)

(12) Forster, F. Z. Elektrochem., **13**, 414 (1907)

(13) Kornfeil, F. Proceedings of the 12th Annual Battery Research and Development Conference, U.S. Army Signal Corps, 1958.

(14) MacArthur, D. M., Journal of the Electrochemical Society, **117**, 424 (1970)

(15) Wagman, D.D, Evans, W.H., Selected Values of Chemical Thermodynamic Properties, CRC Handbook of Chemistry and Physics, 64th ed., Yeast, E.C.(ed.), (1983), page D-50

(16) Beden, B., Lamy, C., Floner, D., and Hahn, F., Electrochimica Acta, **32**, 1631 (1987)

(17) Sandoval, R., Schrebler, R., Gomez, H., Journal of Electroanalytical Chemistry, **210**, 287 (1986)

(18) Briggs, G.W.D., Fleischmann, M., Transactions of the Faraday Society, **67**, 2397 (1971)

(19) Schrebler-Guzman, R.S., Vilche, J.R., Arvia, A.J., Journal of the Electrochemical Society, **125**, 1578 (1978)

(20) Beden, B., Floner, D., Leger, J.M., and Lamy, C., Surface Science, **162** , 822 (1985)

(21) Wagner, F. T., Moylan, T. E., Journal of the Electrochemical Society, **136**, No. 9, 2498 (1989)

(22) MacDougall, B. and Cohen, M., Journal of the Electrochemical Society, **121**, 1152 (1974)

(23) Brundle, C. and Carley, A., Faraday Disc. Chem. Soc., **60**, 51 (1975).

(24) Marcus, Y., Journal of Pure and Applied Chemistry, **55**, No. 6, 977 (1983)

(25) Electrodeposition & Corrossion Processes, J. M. West, Ed., Van Nostrand Reinhold, (1970), p 112

(26) The Corrosion and Oxidation of Metals, U. R. Evans, Ed., Arnold, (1960), p 252

(27) Graham, M.J., Caplan, D., Cohen, M., Journal of the Electrochemical Society, **119**, 879 (1972)

(28) Crooks, R.M., Bard, A.J., Journal of Physical Chemistry, **91**, 4058 (1987)

(29) Lasia, A., 72nd Canadian Chemical Conference and Exhibition, Abstract 703. (1989)

VITA

Surname: Hennig Given Names: Darren Lewis

Place of Birth: Edmonton, AB Date of Birth: 20 June, 1965

Educational Institutions Attended:

University of Victoria	Sept. 1985 to Aug. 1990
Okanagan College	Sept. 1983 to Apr. 1985

Degrees Awarded:

B.Sc. (Honours)	University of Victoria	1987

Scholarships and Awards:

B.C. Provincial Scholarship	1983
Credit Union Bursary	1983
NSERC Student Summer Fellowship	1987
2nd Place, 3rd annual CIC Student Symposium	1987
2nd Place, 4th annual CIC Student Symposium	1988
1st Place, 5th annual CIC Student Symposium	1989

PARTIAL COPYRIGHT LICENCE

I hereby grant the right to lend my thesis (or dissertation) to users of the University of Victoria Library, and to make single copies only for such users or in response to a request from the Library of any other university, or similar institution, on its behalf or for one of its users. I further agree that permission for extensive copying of this thesis for scholarly purposes may be granted by me or a member of the University designated by me. It is understood that copying or publication of this theses for financial gain shall not be allowed without my written permission.

Title of Thesis/Dissertation: Electrochemical Studies of Oxide-Free Nickel Surfaces

Author [redacted]

D.L. HENNIG
(Name in Block Letters)

28 August, 1990
(Date)